TECHNICAL NOTES

NATIONAL ADVISORY COMMITTEE FOR AERONAUTICS

No. 896

ROUND HEAT-TREATED CHROMIUM-MOLYBDENUM-STEEL TUBING UNDER COMBINED LOADS

By William R. Osgood
National Bureau of Standards

July 1943

NATIONAL ADVISORY COMMITTEE FOR AERONAUTICS

TECHNICAL NOTE NO. 896

ROUND HEAT-TREATED CHROMIUM-MOLYBDENUM-STEEL TUBING UNDER COMBINED LOADS

By William R. Osgood

SUMMARY

The results of tests of round heat-treated chromium-molybdenum-steel tubing are presented. Tests were made on tubing under axial load, bending load, torsional load, combined bending and axial load, combined bending and torsional load, and combined axial, bending, and torsional load. Tensile and compressive tests were made to determine the properties of the material. Formulas are given for the evaluation of the maximum strength of this steel tubing under individual or combined loads.

The solution of an example is included to show the procedure to be followed in designing a tubular cantilever member to carry combined loads.

INTRODUCTION

Some of the tubular members, such as the landing gear, used in aircraft are subjected to combined axial, bending, and torsional loads. The design of such members requires a knowledge of their strength under various combinations of these loads. For a given loading any of the stresses within the elastic range may be computed; but these stresses will give little or no information as to the nearness of failure, which occurs in the plastic range. To predict plastic failures theoretically for any but the simplest of cross sections and the simplest of stress-strain diagrams is an insuperable task. In order, therefore, to estimate the strength at failure under combined loading of practical shapes made of practical materials, such shapes must be tested to failure under the desired conditions of loading.

The interest of the Bureau of Aeronautics, Navy Department, in the strength of round heat-treated chromium-

molybdenum-steel tubing under combined loads led to the transfer of funds to the National Bureau of Standards for an investigation of the subject. Most of the tests previously made under combined loading have been made on extremely thin sections, so that the results are not applicable to the relatively thick sections that are of primary interest. Moreover, no tests of heat-treated chromium-molybdenum-steel tubing are known to be available.

The plan of the investigation consists of a series of tests under axial load, bending load, and torsional load alone, a series under axial load combined with bending load, a series under bending load combined with torsional load, and finally, a series in which axial load, bending load, and torsional load act simultaneously. It was not possible to make tests under torsional load combined with axial load because the clear distance ((6 diam.) between loading points would have been so great in order to get away from local effects that the resulting length of the specimen would have made large bending stresses unavoidable.

The Bureau is indebted to the Summerill Tubing Company for donation of the tubing.

The author wishes to acknowledge the help received from various members of the Engineering Mechanics Section, particularly from Mr. J. Southall Noble who, assisted in the most difficult series of the tests: namely, those under combined axial, bending, and torsional loads. Mr. Noble's care and anticipation of things to be done were of inestimable value in obtaining such success as was obtained.

MATERIAL AND TESTS OF MATERIAL

The material was round, heat-treated, S.A.E. X4130 tubing. The lowest 0.002-offset tensile yield strength of the material tested was 155,000 pounds per square inch, the lowest tensile strength was 164,000 pounds per square inch, and the lowest elongation in 2 inches of the full tube was 5 percent. Thus, the tubing did not all comply with the requirements for tubing in any one physical condition specified in Army-Navy Aeronautical Specification AN-WW-T-850a: Tubing; Steel, Chrome-Molybdenum (X4130), Seamless. Except for the requirement for elongation in 2 inches, however, all the tubing complied with the required

mechanical properties for (HT-150) tubing, minimum yield strength of 135,000 pounds per square inch, minimum tensile strength of 150,000 pounds per square inch.

The nominal cross-sectional properties of the tubes are given in table I. The letter in the first column is the symbol used to identify the size of the tubing - that is, outside diameter (d) and thickness of wall (t).

At least one tensile specimen and one compressive specimen were taken from each tube.

All specimens were marked with symbols that indicated by an initial digit the tube from which the specimen was cut, by a letter (H) the fact that the material was heat treated, by another letter the nominal size of the tube, then by one or more letters following a dash, the type of test to which the particular specimen was to be subjected, and by a final digit different specimens intended for the same type of test. The letters indicating the nominal sizes of the tubes are given in table I. The letters A, B, and T were used to indicate axial, bending, and torsional loading, respectively, except that To was used for pure torsion and T by itself was used for tension. The letter C was used to indicate compressive specimens (axial loading) for which stress-strain data were obtained. For example, specimen 3HA-BT1 was cut from tube 3 of heat-treated chromium-molybdenum steel, H, having the nominal size $1\frac{1}{2}$ inches diameter by 0.120 inch thick, A (table I), and was tested in combined bending and torsion, BT. The final 1 distinguished this specimen from other specimens cut from tube 3HA, also tested in combined bending and torsion, such as 3HA-BT and 3HA-BT2. Specimens 3HA-T, 3HA-C, and 3HA-To would be tensile, compressive, and torsional specimens, respectively, cut from tube 3HA. Specimen 3HA-A would be a specimen like 3HA-C, for which only the crinkling strength, not stress-strain data, would be obtained.

Measured dimensions of specimens were used in all computations. In general, alternate specimens in a tube were measured. The lengths, minimum and maximum thicknesses at each end, and outside diameters at the middle were measured. Most of the measured specimens were also weighed. The cross-sectional areas were in most cases computed from the weights, the lengths, and the densities; otherwise, the areas were computed from the average measured diameter and the average measured thickness of each specimen. Similarly, the average thicknesses and the section moduli were determined from the computed cross-

sectional areas and the measured outside diameters unless the specimens were not weighed, in which case these quantities were determined directly from the measured dimensions. The thicknesses, cross-sectional areas, and section moduli of specimens adjacent to or between measured specimens were taken equal to those of adjacent specimens or they were interpolated between values for measured specimens.

Tensile tests were made of "full-tube" specimens in suitable testing machines. Compressive tests were made as described in reference 1, except that new hydraulic testing machines were used. The three shortest specimens shown in figure 1(a) are compressive specimens after test. One of these specimens has still attached to its ends the Wood's-metal castings used to secure somewhat more uniform conditions at the ends of compressive specimens and of crinkling specimens. As in the earlier tests (reference 1) the machines were not particularly well adapted for compressive tests, many of the specimens, although only four diameters long, showing evidence of bending at failure. The bending may have been due to tilting of the platen caused by yielding of the packing between ram and cylinder of the testing machine. It is believed that the ram of a hydraulic machine designed for compressive tests should be a close fit in the cylinder — close enough to dispense with packing. Bending in the specimens may possibly also have been induced by exceeding the critical loads of the testing machines. An excellent discussion of this phenomenon may be found in reference 2.

Strains up to approximately 0.01 were measured with a Ewing extensometer on a 2-inch gage length in all tensile and compressive specimens except one tensile specimen. Two Tuckerman strain gages on 2-inch gage lengths were used on this specimen.

The moduli of elasticity were obtained from the stress-strain data by means of deviation curves (reference 3). Two tensile yield strengths were obtained for each tensile specimen from stress-strain curves: namely, the 0.002-offset yield strength and the 5/7 E-secant yield strength. The offset yield strength is well known, the secant yield strength is discussed in reference 4. It is the stress at the intersection with the stress-strain curve of a straight line through the origin having a slope $5/7\,E$, where E is Young's modulus. The 5/7 E-secant yield strength was obtained for each compressive specimen from stress-strain curves. Figure 2 shows typical stress-strain curves. The

short cross lines near the tops of the curves indicate the yield strengths, the left-hand lines of the tensile diagrams indicating the offset yield strengths. The mechanical properties are given in table II.

In most (18) of the tubes a compressive specimen was cut adjacent to a tensile specimen and it was therefore possible to compare the compressive with the tensile properties unaffected by wide variations along the tube. In an attempt to correlate the compressive yield strength with tensile properties, various quantities were plotted against each other. It was found that the compressive yield strength, S, could be predicted from the tensile strength, T, both in pounds per square inch, by the linear relation

$$S = 7/6\ (T - 30{,}000),\ 174{,}000 < T < 194{,}000 \qquad (1)$$

Figure 3 shows the plotted values and the line represented by equation (1). The maximum difference between an observed compressive yield strength and the yield strength computed from the formula was 7350 pounds per square inch or 4.2 percent; the observed yield strength was lower by this amount. When the compressive yield strength was plotted against the secant tensile yield strength, a greater scatter was found than in figure 3.

Some wide variations in mechanical properties were found along some of the tubes and may have existed in others. At one end of tube 2HY the secant yield strength and the tensile strength were 156,000 and 164,000 pounds per square inch, respectively, and about 100 inches from this end they were 173,000 and 187,000 pounds per square inch, respectively. The tensile specimen from tube 4HD was cut from an end and had a tensile strength of 171,000 pounds per square inch. The adjacent compressive specimen had a yield strength of 181,000 pounds per square inch. This yield strength was so much higher than would be expected from the results of the other tests, figure 3, that the tensile strength is believed to have been abnormally low. The values for tube 4HD were not used in obtaining equation (1) and are not plotted in figure 3. Omitting them in predicting compressive yield strength is on the safe side. One other tube, 1HY, had a tensile specimen cut from one end. This specimen had a tensile strength of 168,000 pounds per square inch, and there are indications,

which will be discussed subsequently, that this value is also abnormally low. Two compressive specimens from tube 2HD were about $56\frac{1}{2}$ inches apart, center to center. The compressive yield strengths of these specimens differed by 184 pounds per square inch per inch of distance between them, or over 0.1 percent per inch.

AXIAL TESTS

The axial tests consisted of the compressive tests and a few crinkling tests, the only difference between these two categories being that stress-strain data were not taken on the crinkling specimens. Three compressive specimens after test are shown in figure 1(a).

The results of the axial tests are given in table III. The symbols d and t are the outside diameter and the thickness of the wall, respectively, of the specimen. The crinkling strength, f_A, is the maximum axial load sustained by the specimen divided by its cross-sectional area. The lower group of points in figure 4 shows the relation between d/t and f_A. One point, enclosed in braces (specimen 4HY-C), is in question because the specimen was recut from a specimen tested under combined axial, bending, and torsional loading. Otherwise, the scatter in figure 4 is to be attributed largely to variations in the properties of the material, particularly the compressive yield strength. As discussed in reference 1, the scatter can be much reduced by plotting $\sigma_A = \frac{f_A}{S}$ against $\frac{1}{\delta} = \frac{Et}{Sd_m}$, where d_m is the mean diameter, $d - t$, of the specimen. Values of $1/\delta$ and σ_A are given in table III and are plotted as the lower group of points in figure 5. The compressive yield strengths of 28 of the compressive specimens (all except 4HY-C) were known accurately, and the relation between σ_A and $1/\delta$ for these specimens can be given by

$$\sigma_A = 0.67 + 0.112\frac{1}{\delta} - 0.0099\frac{1}{\delta^2} + 0.0003\frac{1}{\delta^3}, \qquad 4 < \frac{1}{\delta} < 16 \quad (2)$$

with a maximum deviation in σ_A of 0.020 or less than 2 percent. The data in themselves are not considered to

warrant the refinement implied in equation (2), but the use to be made of the data in subsequent estimates of compressive yield strengths and in the combined tests made it seem desirable to approximate as closely as reasonably possible by means of an analytical expression. The curve represented by equation (2) is shown in figure 5. To one familiar with the type of results depicted, the occurrence of a point of inflection may cause some skepticism, but a ready explanation may be given. The compressive stress-strain curves of the HA material ($1/\delta$ between 15 and 16) all were appreciably steeper in the plastic range than those of the other material. Consequently, in accordance with Geckeler's theory (references 1 and 5), higher loads at failure would be expected from the HA material than if its stress-strain curves had been less steep in the plastic range, specifically, less steep at the stress at failure.

Specimens 1HL-A and 1HL-A1 were taken between two compressive specimens, and their moduli of elasticity and their yield strengths were estimated by linear interpolation between the values found for the compressive specimens. The points representing specimens 1HL-A and 1HL-A1 in figure 5 are enclosed in brackets. The moduli of elasticity of the other crinkling specimens were assumed equal to that of the compressive specimen of the tube from which they came. Their yield strengths were estimated, as explained in appendix A, from equation (2) and the maximum variation in yield strength found between two compressive specimens from the same tube, namely 184 pounds per square inch per inch, all tubes with two compressive specimens being considered. The points representing these specimens in figure 5 are enclosed in parentheses. Finally, the point representing specimen 4HY-C is enclosed in braces, because it is questionable as mentioned previously, and should be left out of consideration. This point fortunately falls above the curve, and its omission is therefore on the safe side.

BENDING TESTS

The bending tests were made as described in reference 1, the specimens being loaded symmetrically at two sections and essentially the same apparatus with a few practical modifications being used. Three bending specimens after test are shown in figure 1(b).

The results of the bending tests are given in table IV. The modulus of rupture, f_B, was computed from the familiar flexure formula,

$$f_B = \frac{\overline{M}}{Z}$$

where $\overline{M}$ is the maximum bending moment sustained, and Z is the section modulus of the cross-sectional area. The upper group of points in figure 4 shows the relation between d/t and f_B. As in the axial tests, the scatter is pronounced and somewhat more marked than in those tests. It seems likely that variation in the mechanical properties circumferentially as well as longitudinally and from tube to tube enter the picture here. If, for example, the compressive yield strength of the part of the specimen in compression happened to be relatively low, the bending strength of that specimen would be lower than if it had been tested with this part in some other position. Without a knowledge of the circumferential variation of the mechanical properties nothing can be done to correct for their effects, but something can be done about that part of the scatter caused by variation in the average compressive yield strength between specimens, at least to the extent to which the yield strengths of the individual specimens are known. Again, as in reference 1, $\sigma_B = \frac{f_B d_m}{Sd}$ is plotted against $\frac{1}{\delta} = \frac{Et}{Sd_m}$. Values of $1/\delta$ and σ_B are given in table IV and are plotted as the upper group of points in figure 5. Values of the moduli of elasticity and the compressive yield strengths were estimated as explained in appendix A. Two specimens, 2HF-B and 2HF-B1, were more than 100 inches away from the nearest specimen for which a yield strength could be estimated with some degree of assurance and, in view of the large possible variation in yield strength in this length, about 10 percent, the points representing these specimens in figure 5 have been enclosed in braces. They are considered unreliable. Specimen 2HF-B (the lower point in the figure), moreover, was cut from an end of the tube and may well have had an abnormally low tensile yield strength and possibly a somewhat lowered compressive yield strength. One other point is conspicuous: namely, the one representing specimen 3HY-B. This specimen also was cut from an end of the tube, but because it was less

than 100 inches from a specimen with a fairly reliably known yield strength, it did not seem justifiable to throw it out, even though its yield strength was not so well known as was to be desired. Other low points in figure 5 similarly represent specimens cut from ends of tubes; but because not all specimens cut from ends give low values of σ_B, a considerable number of additional tests would be necessary to establish a relation between $1/\delta$ and σ_B that could be said to be definitely better than one based on the available data. If only specimens 2HF–B and 2HF–B1 are neglected, the relation between σ_B and $1/\delta$ can be given by

$$\sigma_B = 0.7 + 0.16\,\frac{1}{\delta} - 0.015\,\frac{1}{\delta^2} + 0.000485\,\frac{1}{\delta^3}, \quad 4 < \frac{1}{\delta} < 16 \qquad (3)$$

with a deviation in σ_B of 6.5 percent for specimen 3HY–B and otherwise with a maximum deviation of 4.5 percent. The two curves in figure 5 probably should have the same shape: for example, if one of them is markedly concave downward over part of the range of $1/\delta$ and concave upward over the rest of the range, one would expect the other to be so also, although the point of inflection might not come at exactly the same $1/\delta$. If all specimens cut from ends of tubes were neglected and a fair curve to represent the results were drawn, the curve would follow the shape of the curve representing crinkling strength less closely than the curve shown in figure 5. The curve of crinkling strength is well established and the curve of bending strength should follow it. It therefore seems that equation (3) is at least as good as, and probably better than, a relation obtained by neglecting specimens cut from the ends of tubes. Including these specimens is safe because σ_B is lowered when they are included.

As in the case of the axial tests, the refinement implied by equation (3) is not justifiable on the basis of the data alone. The use to be made of these data in the analysis of the combined tests later, however, made it seem desirable to approximate closely to them. The rise in σ_B at high values of $1/\delta$ is to be explained in the same way as the rise in σ_A at high values of $1/\delta$.

TORSIONAL TESTS

The torsional tests were made as described in reference 6. Three torsional specimens after test are shown in figure 1(c).

The results of the torsional tests are given in table V. The modulus of rupture in torsion, f_T, was computed from the formula

$$f_T = \frac{M_T}{2Z}$$

where M_T is the maximum twisting moment. The relation between d/t and f_T is shown in figure 6. The scatter in the points is due primarily to variation in the mechanical properties of the specimens. The most significant property in this respect is probably the compressive yield strength. In order to introduce this quantity in a rational manner, the solution for two-lobed buckling of a long, thin elastic cylindrical shell under torsion is examined. Timoshenko (reference 7) finds the shearing stress $f_m = f_T \frac{d_m}{d}$ at the instant of buckling to be given by

$$f_m = \frac{2E}{3(1-\nu^2)^{\frac{3}{4}}} \left(\frac{t}{d_m}\right)^{\frac{3}{2}}$$

The theory for plastic buckling is not known to have been worked out, but it is probable that, as in Geckeler's theory (reference 1), the double-modulus would appear on the right side of the equation and that a relation could be found between the variables $\frac{1}{\delta_s} = \left(\frac{E}{S}\right)^{\frac{2}{3}} \frac{t}{d_m}$ and $\tau_T = \frac{f_T}{S} \frac{d_m}{d}$ which would be the same for all materials having affinely related stress-strain curves (S necessarily being the secant yield strength). For the elastic case the relation would be

$$\tau_T = \frac{2}{3(1-\nu^2)^{\frac{3}{4}}} \left(\frac{1}{\delta_s}\right)^{\frac{3}{2}} \qquad (4)$$

The preceding considerations suggest that τ_T be plotted against $\frac{1}{\delta_s}$. Values of these nondimensional variables are given in table V and have been plotted in figure 7. Values of the moduli of elasticity and the compressive yield strengths were estimated as explained in appendix A. The relation between $\frac{1}{\delta_s}$ and τ_T can be given by

$$\tau_T = 0.06\left(\frac{1}{\delta_s} - 0.8\right) + 0.5, \quad 0.8 < \frac{1}{\delta_s} < 3.2 \qquad (5)$$

with a maximum deviation of 5.5 percent. Equation (4) for elastic buckling, with $\nu = \sqrt{1 - \frac{64}{75}\sqrt{\frac{4}{3}}} \approx 0.25$, is also represented in figure 7 by the dotted curve.

COMBINED AXIAL AND BENDING TESTS

The combined axial and bending tests were made in a horizontal testing machine. Figure 8 shows the setup for a test. The ends of the specimen were plugged with snug-fitting plugs, shown at the right in figure 9. The outer ends of the plugs contained hardened steel inserts, shown in the top plug in figure 9, and were turned to fit closely in the ball bearing shown in the pillow-block assembly in figure 9. When a plug was pushed into one of the ball bearings, its hardened insert bore on a half-inch steel ball in the pillow-block assembly, shown on the axis of the ball bearing in figure 9. The point of contact between the hardened insert and the ball was accurately located on the axis of rotation of the pillow blocks. The capacity of one of the pillow-block assemblies was 20,000 pounds.

Tests were made as follows. The pillow-block assemblies were securely fastened to the heads of the testing

machine with the axes of the pillow blocks horizontal and accurately parallel (fig. 8). Loading clamps (reference 1) were applied to symmetrically situated sections of the specimen not less than about 6 diameters apart, and the plugs mentioned previously were pushed into the ends of the specimen. The specimen was then transferred to the testing machine, the outer ends of the plugs being inserted in the ball bearings of the pillow-block assemblies; one plug was inserted first and the head of the machine was then moved up and the other plug inserted. An initial axial load of a few hundred pounds, depending on the size of tho specimen, was applied.

A deflectometer (figs. 8 and 10) was attached to the middle of the specimen. Since the middle of the specimen assumed a pronouncedly oval shape at failure, it was thought desirable in the interests of accuracy to measure the deflection of a horizontal diameter. The deflectometer was therefore attached to the specimen by means of two hard conical points in the ends of a clip that snapped into diametrically opposite prick-punched holes in the specimen. The clip was fastened to a steel scale sliding in a slotted frame having a vernier. Deflections could be read directly to 0.002 inch. The deflectometer was eminently satisfactory. It could be removed from the specimen and replaced with a change in reading not greater than 0.001 inch and, with the deflectometer attached, the specimen could be rotated about its axis through several degrees with a change in reading of the deflection not exceeding 0.001 inch.

A dial gage, shown in figure 8, was attached to measure the motion of the pillow-block assemblies toward each other as axial load was applied.

With the deflectometer and the dial gage attached, initial readings of these two instruments were taken, and then transverse load was applied to the specimen by means of hangers, an equalizer, and dead weights (fig. 8). The axial load was then increased gradually until a maximum was passed, and frequent readings were taken of the axial load, the deflectometer, the dial gage, and the distance between loaded sections. Three specimens after failure under combined axial and bending load are shown in figure 1(d).

The axial stress, $f_a = P/A$, was computed as the axial

load, P, at failure divided by the cross-sectional area, A, of the specimen. The bending stress was computed from the flexure formula

$$f_b = \frac{M}{Z}$$

where M is the maximum bending moment produced by the transverse load and the axial load. The moment arm of the reaction for determining the bending moment produced by the transverse load was computed from the initial distance between the axis of a set of pillow blocks and the adjacent loaded section, corrected for shortening from the reading of the dial gage and the distance between the loaded sections. The bending moment produced by the axial load was the product of the axial load and the deflection of the middle of the specimen.

Values of f_a and f_b are given in table VI. If f_a and f_b were to be plotted against each other, the points would be found to scatter about a series of curves representing different values of d/t. The scatter could be reduced by plotting $\sigma_a = \frac{f_a}{S}$ and $\sigma_b = \frac{f_b}{S}\frac{d_m}{d}$ against each other. It was found that the effect of different values of d/t could be much reduced, and perhaps eliminated within the experimental error, by plotting $\frac{\sigma_b}{\sigma_B}$ against $\frac{\sigma_a}{\sigma_A}$, where σ_B and σ_A are computed from equations (3) and (2), respectively. Values of $\frac{1}{\delta}$ for computing σ_A and σ_B, and values of σ_a, σ_b, $\frac{\sigma_a}{\sigma_A}$, and $\frac{\sigma_b}{\sigma_B}$ are given in table VI. The moduli of elasticity and the compressive yield strengths of the individual specimens were estimated as explained in appendix A. The ratio $\frac{\sigma_b}{\sigma_B}$ plotted against the ratio $\frac{\sigma_a}{\sigma_A}$ is shown in figure 11. This figure still shows appreciable scatter, some of which is no doubt due to the uncertainty in the yield strengths, almost surely so for the 2HY- specimens. The order of these

specimens in the tube was 2HY-T1, -AB, -AB1, -AB2, -AB3, -AB4, -T. Specimen 2HY-T was an end specimen with an abnormally low tensile strength. The compressive yield strength estimated from it (see appendix A) would consequently also be abnormally low, so that, in interpolating the compressive yield strengths of the specimens between 2HY-T1 and 2HY-T, abnormally low values would be obtained at the 2HY-T end of the interval. The relative positions of the points in figure 11 representing the 2HY- specimens reflect this situation, the points for specimens 2HY-AB2, -AB3, and -AB4 being quite out of line with the points for specimens 2HY-AB and 2HY-AB1. Again, specimen 1HD-AB, taken next to a crinkling specimen for which the yield strength is fairly well known, falls in line fairly well in figure 11; whereas specimens 1HD-AB1 and 1HD-AB2 with questionable yield strengths are out of line. Some of the scatter in figure 11 is also due to the uncertainty in the moment of the axial load. As the maximum axial load is approached, the deflection increases rapidly relative to the axial load, and it is difficult to say just what the deflection is at the maximum axial load. Frequently no change in axial load is indicated by the testing machine for a considerable variation in deflection (several tenths of an in.), particularly in the case of the relatively thick specimens. It seems quite possible, almost probable, that the d/t-effect still showing in figure 11 is due to the uncertainty in the moment of the axial load. The tendency in the laboratory was to underestimate this moment (on the side of safety), and, as mentioned, the error in the estimate was likely to be greater for the thick specimens. If this is so, the points representing the HA- and the HL-tubes should be moved up. This difficulty of determining the maximum axial load and the accompanying deflection is inherent in any testing machine that does not follow through with the load. Dead-weight loading would be required to overcome it satisfactorily. The points in figure 11 have been approximated to by the equation

$$\left(\frac{\sigma_a}{\sigma_A}\right)^{\frac{8}{10}} + \left(\frac{\sigma_b}{\sigma_B}\right)^{\frac{8}{10}} = 1, \qquad \frac{\sigma_a}{\sigma_A} < 1, \tag{6}$$

and the curve represented by the equation is shown in the figure. The curve favors low values of σ_a/σ_A and tends to be conservative in general. In most practical cases in which combined axial and bending loads occur, it is

believed that the axial stress will be smaller than the maximum bending stress, so that the upper half of the curve is perhaps more important than the lower half.

COMBINED BENDING AND TORSIONAL TESTS

The combined bending and torsional tests were made as shown in figures 12 and 13. The tests were made essentially in the same way as the bending tests, except that torsion was introduced by clamping split pulleys to the specimen at the loaded sections and loading through wire ropes leaving the pulleys on opposite sides of the specimen. Pulleys with diameters of 12 and 30 inches were used (the 30-in. pulleys are shown in the figures) and, by varying the span, various combinations of bending moment and twisting moment could be secured. Great difficulty was experienced in gripping the specimen in torsion. The grips shown in figure 14 were finally designed and worked satisfactorily. Snug-fitting plugs each $1\frac{1}{4}$ inches long were pushed into the specimen to the positions at which the grips were to be applied. The specimen was placed in one of the grips, and three cylindrical segments, shown at the extreme right and left of the figure, were inserted in the outer end of the grip symmetrically around the circumference of the specimen. Three serrated hard steel wedges 1 inch wide, shown in the middle of the figure, were then inserted between the specimen and the inner end of the grip at the position of one of the plugs previously pushed into the specimen. These wedges slid on the three plane surfaces shown at the inner end of the left-hand grip in the figure. They were pushed tightly against the specimen by means of fine-thread setscrews. By also tightening the cylindrical segments against the specimen by means of setscrews, the grip was securely held on the specimen with its axis and that of the specimen colinear. The other grip was attached in the same way, opposite hand. These grips replaced the grips first used, shown in figures 12 and 13, and are shown in figure 15 attached to a specimen. Three combined bending and torsional specimens after failure are shown in figure 1(e). It is interesting to compare the orientations of the buckles in two of the specimens with those of the bending and torsional specimens. In the bending and the torsional specimens the buckles, when they appeared, formed at right angles and at approximately 45°, respectively, to the axis

of the specimen. In the combined bending and torsional specimens the buckles appeared at an intermediate inclination, as would be expected.

The bending stress, f_b, and the torsional stress, f_t, were computed from the formulas $f_b = \frac{\overline{M}}{Z}$ and $f_t = \frac{M_t}{2Z}$, respectively, where $\overline{M}$ and M_t are the maximum bending moment and maximum twisting moment. Values of f_b and f_t are given in table VII. When f_b and f_t are plotted against each other, the points are found to scatter about a series of curves representing different values of d/t. As in the combined axial and bending tests the scatter could be reduced by plotting

$$\sigma_b = \frac{f_b d_m}{Sd} \quad \text{and} \quad \tau = \frac{f_t d_m}{Sd}$$

against each other. As found previously, the effect of the ratio d/t can be eliminated within the experimental error by plotting τ/τ_T against σ_b/σ_B, where τ_T and σ_B are computed from equations (5) and (3), respectively. Values of $1/\delta$ and $1/\delta_s$ for computing σ_B and τ_T, and values of σ_b, τ, σ_b/σ_B, and τ/τ_T are given in table VII. The moduli of elasticity and the compressive yield strengths of the individual specimens were estimated as explained in appendix A. The values of τ/τ_T plotted against σ_b/σ_B are shown in figure 16. Although this figure still shows appreciable scatter, most of it can be explained by variations in yield strength along the length of the tubing. The specimens of tube 3HY were cut in the order 3HY–BT, –BT1, –BT2, –BT3, –T, –C, –BT4, –BT5, –B. The order of specimens in figure 14 arranged according to increasing values of σ_b/σ_B is 3HY–BT1, –BT, –BT2, –BT3, –BT4, –BT5. It was necessary in the absence of other information to assume the compressive yield strength of all of these specimens to be that of the compressive specimen, 3HY–C. It seems rather evident, however, from the low value of $\frac{\sigma_b}{\sigma_B}$ (0.123) and the accompanying high value of $\frac{\tau}{\tau_T}$ (1.072) for specimen 3HY–BT1

that the yield strength of this specimen was greater than that of the compressive specimen. It is hardly conceivable that τ/τ_T could exceed 1. Since specimen 3HY–BT1 was near the end of the tube and probably had a relatively high yield strength, the yield strength may be assumed to have decreased from this end of the tube to the other end. If this assumption is made, specimens 3HY–BT4 and 3HY–BT5 which now appear to have low values of σ_b/σ_B and τ/τ_T and were on the other side of the compressive specimen 3HY–C, would have lower yield strengths than assumed, and the points representing them would be raised and moved to the right in figure 16. The other values for the 3HY-specimens would also lie nearer the curve. Another tube exhibiting anomalous behavior in figure 16 is 2HD. Specimen 2HD–BT3 was cut adjacent to a compressive specimen and between two such specimens; its compressive yield strength should therefore be known rather accurately, and it appears to be satisfactorily represented in figure 16 (the point (0.099, 1.006)). The other three 2HD specimens, however, were cut between a compressive specimen and the end of the tube, and none of them was adjacent to the compressive specimen. Their yield strengths were all assumed to be that of the compressive specimen. It seems probable, from the high value of $\frac{\tau}{\tau_T}$ (1.047) that this assumption was in error and that their yield strengths were actually higher than assumed. Finally, values for specimens 3HF–BT and 3HF–BT1 gave rather high values. These two specimens were cut from the same relative position in the tube as the three 2HD specimens just discussed, and their yield strengths similarly may not have been reliable. The compressive yield strengths of the remaining specimens could, in general, be estimated more reliably than those of the specimens that have been mentioned. All the errors in the previous discussion have tacitly been attributed to errors in τ and σ_b. It should be remembered, however, that τ_T and σ_B also contain errors and that these errors also enter the problem, although in an unknown way.

When consideration is taken of the anomalous points in figure 16, the relation between σ_b/σ_B and τ/τ_T can be given reasonably by

$$\left(\frac{\sigma_b}{\sigma_B}\right)^{\frac{5}{2}} + \left(\frac{\tau}{\tau_T}\right)^{\frac{5}{2}} = 1 \qquad (7)$$

The curve represented by this equation is shown in figure 16. With the apparatus at hand combinations of smaller values of τ/τ_T and larger values of σ_b/σ_B than those shown could not be obtained, but, since any curve representing the results of tests must go through the point (1.0, 0), the uncertainty in the lower portion of the curve adopted is not considered to be excessive.

COMBINED AXIAL, BENDING, AND TORSIONAL TESTS

The final series of tests, under combined axial, bending, and torsional loads, were made as shown in figure 15. The setup is similar to that used in the combined axial and bending tests, but the transverse loads were applied by dead weights suspended from opposite sides of two pulleys, thus producing torsion as well as bending. The pulleys, 36 inches in diameter for these tests, played the same role as the pulleys in the combined bending and torsional tests. The procedure for making a test was practically the same as that for making a combined axial and bending test. The vernier on the deflectometer was read with a telescope. Three specimens after failure are shown in figure 1(f).

The axial stress, $f_a = \frac{P}{A}$, was computed as the axial load, P, at failure divided by the cross-sectional area, A, of the specimen. The bending stress f_b and the torsional stress f_t were computed from the formulas $f_b = \frac{M}{Z}$ and $f_t = \frac{M_t}{2Z}$, respectively, where M was the maximum bending moment and M_t was the (constant) twisting moment. Values of f_a, f_b, and f_t are given in table VIII. The previous two series of tests under combined load indicated that the significant variables to be correlated were σ_a/σ_A, σ_b/σ_B, and τ/τ_T. These quantities were therefore computed for this last series of tests. Values of $1/\delta$ and $1/\delta_s$ for computing σ_A, σ_B, τ_T from equations (2), (3), and (5),

values of σ_a, σ_b, and τ; and values of σ_a/σ_A, σ_b/σ_B, and τ/τ_T are given in table VIII. If the last three variables are assumed to form a consistent set for all the conditions of the tests, a surface which adequately represents them must be found. The surface must cut the σ_a/σ_A, σ_b/σ_B - plane and the σ_b/σ_B, τ/τ_T-plane in the curves of equations (6) and (7), respectively. Several surfaces were tried and, since the uncertainty in σ_b/σ_B was far greater than that in σ_a/σ_A and τ/τ_T, observed and computed values of σ_b/σ_B were compared. The surface that was finally selected as most nearly representative of the test data was

$$\frac{\left(\frac{\sigma_b}{\sigma_B}\right)^{\frac{5}{2}}}{\left[1-\left(\frac{\sigma_a}{\sigma_A}\right)^{\frac{9}{10}}\right]^{\frac{25}{9}}}+\frac{\left(\frac{\tau}{\tau_T}\right)^{\frac{5}{2}}}{\left(1-\frac{\sigma_a}{\sigma_A}\right)^{\frac{5}{2}}}=1, \qquad \frac{\sigma_a}{\sigma_A}<1 \qquad (8)$$

The traces of this surface on the coordinate planes are shown in figure 17. Of the 21 sets of observed values of σ_a/σ_A, σ_b/σ_B, and τ/τ_T nine sets fell inside the surface and twelve fell outside. There was a distinct tendency for the specimens with low values of d/t to fall inside the surface. This tendency may represent a real d/t - effect but, as explained in the discussion of the combined axial and bending tests, it may merely represent the greater uncertainty in estimating the bending moment arising from the axial load. In the case of the thick specimens the moment was estimated low rather than high. An attempt was made to improve the estimate by plotting readings of axial load against deflection and picking the maximum load from a smooth curve drawn through the points, but near the maximum load the curve was so flat for a large range of deflection that a reliable maximum and corresponding deflection could not be read off. The only answer to this problem would seem to be dead-weight application of axial load, an expensive procedure.

APPLICATION TO (HT-180) MATERIAL

All the results of the investigation have been given in nondimensional form. This form, which is best suited for presenting test data, is not convenient for practical use, and it remains to apply the information obtained in terms of the actual material and its dimensions. Although, as stated at the beginning of this report, except for the requirement for elongation, all the material complied with the required mechanical properties for HT-150 tubing, nevertheless the material is more nearly representative of the HT-180 tubing, minimum required yield strength of 165,000 pounds per square inch and minimum required tensile strength of 180,000 pounds per square inch. It will therefore be assumed that it does represent HT-180 tubing. In order to apply the various equations representing the results, the modulus of elasticity and the compressive yield strength to be expected of material just complying with the specification must be known. The average modulus found for the compressive specimens was $E = 29.5 \times 10^6$ pounds per square inch. The compressive yield strength, S, is obtained from equation (1) (T = 180,000) as 175,000 pounds per square inch. With these values of E and S the several equations of the report may be transformed.

The crinkling strength becomes from equation (2)

$$f_A = 117{,}200\left[1 + \frac{28.18}{\frac{d}{t} - 1} - \frac{419.9}{\left(\frac{d}{t} - 1\right)^2} + \frac{2145}{\left(\frac{d}{t} - 1\right)^3}\right], 11.54 < \frac{d}{t} < 43.14 \qquad (9)$$

The curve represented by this equation is shown in figure 4.

The modulus of rupture becomes from equation (3)

$$f_B = \frac{122500\frac{d}{t}}{\frac{d}{t} - 1}\left[1 + \frac{38.53}{\frac{d}{t} - 1} - \frac{608.9}{\left(\frac{d}{t} - 1\right)^2} + \frac{3319}{\left(\frac{d}{t} - 1\right)^3}\right], 11.54 < \frac{d}{t} < 43.14 \qquad (10)$$

The curve represented by this equation is shown in figure 4.

The modulus of rupture in torsion becomes from equation (5).

$$f_T = \frac{79100\frac{d}{t}}{\frac{d}{t} - 1}\left(1 + \frac{4.051}{\frac{d}{t} - 1}\right), \quad 10.54 < \frac{d}{t} < 39.14 \qquad (11)$$

The curve represented by this equation is shown in figure 6.

Equations (6), (7), and (8) for combined loads become simply

$$\left(\frac{f_a}{f_A}\right)^{\frac{9}{10}} + \left(\frac{f_b}{f_B}\right)^{\frac{9}{10}} = 1, \qquad \frac{f_a}{f_A} < 1, \quad (12)$$

$$\left(\frac{f_b}{f_B}\right)^{\frac{5}{2}} + \left(\frac{f_t}{f_T}\right)^{\frac{5}{2}} = 1, \quad (13)$$

$$\frac{\left(\frac{f_b}{f_B}\right)^2}{\left[1 - \left(\frac{f_a}{f_A}\right)^{\frac{9}{10}}\right]^{\frac{25}{9}}} + \frac{\left(\frac{f_t}{f_T}\right)^{\frac{5}{2}}}{\left(1 - \frac{f_a}{f_A}\right)^{\frac{5}{2}}} = 1, \quad \frac{f_a}{f_A} < 1, \quad (14)$$

respectively, where f_a, f_b, and f_t are the components of stress arising from the actual loading, and f_A, f_B, and f_T have the values given by equations (9), (10), and (11) for the particular d/t of the tube being considered. It should be noted that all the equations represent maximum conditions, that is, conditions at failure. In the presence of axial load, f_b must therefore include the bending stress produced by this load since this stress may be considerable at failure. To estimate it requires a knowledge of deflection at failure; use of the deflection under the assumption of elastic conditions will not be safe. The actual deflection is known only for the particular conditions of the tests. Many additional tests would be required to determine this deflection for an appreciable number of other types of loading. It is suggested, therefore, that for other types of loading the actual deflection be considered to bear the same relation to the elastic deflection as the actual deflection of the tested specimens bore to the elastic deflection. Figure 18 shows, in effect, this relation for the specimens tested under combined axial and bending loads. The abscissas are the ratios of the maximum total bending moment M produced

by the transverse load and the axial load, computed by elastic theory (see appendix B), to the maximum bending moment M_b produced by the transverse load alone. The ordinates are the ratios of the observed maximum total bending moment $\overline{M}$ to M_b. A straight line

$$\frac{\overline{M}}{M_b} = 1 + \frac{17}{13}\left(\frac{M}{M_b} - 1\right), \quad 1 < \frac{M}{M_b} < 3.6 \qquad (15)$$

expressing the relation for low values of M/M_b is shown in the figure. The relation is inadequately defined for high values of M/M_b but the equation

$$\frac{\overline{M}}{M_b} = 4.4 + \frac{15}{8}\left(\frac{M}{M_b} - 3.6\right), \quad \frac{M}{M_b} > 3.6 \qquad (15a)$$

may be used if necessary in the absence of other information. If the specimens tested under combined axial, bending, and torsional loads were treated in the same way the points representing them would in general fall below those shown in figure 18. If the data were sufficiently good, it would be possible to draw a series of curves between the lines represented by equations (15) and (15a) and the (dotted) line for the elastic case, $\overline{M}/M_b = M/M_b$ each of these curves representing some condition of torsion; but the data are not good enough.

It should be emphasized that equations (15) and (15a), applied to other conditions of loading than those of the tests or to tubing with stress-strain curves differing widely in shape from those of the tests, are nothing more than arbitrary expressions for reducing Young's modulus to make it possible to estimate the effect of plastic deflections by elastic theory. These equations are substantiated by only a limited number of tests made under special conditions of loading (symmetrical two-point loading) and represent conditions at failure for this type of load. If torsional loads are added, the equations become conservative. Nothing is known as to how good the relation is for other types of bending load. On the other hand, consideration of the whole picture combined with engineering judgment makes it seem that equation (15) may be exploited without too much trepidation.

To design a tubular member subjected to axial load combined with bending load or bending load and torsional load, proceed as follows. Select a trial section, compute M/M_b from the known load and dimensions, and then compute $\overline{M}/M_b$ and thus $\overline{M}$ from equation (15). From this value of $\overline{M}$, compute f_b,

$$f_b = \frac{\overline{M}}{Z}$$

Compare the value so obtained with the allowable value from equation (13) or equation (14). It may be noted that tables of the three-halves powers and the five-halves powers of numbers, such as reference 8, are of material assistance in solving equations (12), (13), and (14). Charts may also be constructed to facilitate the solution of these equations.

Example

It is desired to design a tubular cantilever member to carry an end thrust $P = 16{,}000$ pounds, a bending moment $M_b = 54{,}000$ pound-inches applied at the free end, and a twisting moment $M_t = 25{,}000$ pound-inches applied at the free end. The length l of the member is 52 inches. The modulus of elasticity may be taken as 29,500,000 pounds per square inch.

Try a section 3 inches in outside diameter by 0.120 inch thick. For this section $d/t = 25.0$, $A = 1.086$ square inches, $I = 1.128$ inches^4, $Z = 0.7518$ inch^3. Then

$$f_a = \frac{16000}{1.086} = 14{,}730.$$

and, from equation (9),

$$f_A = 187{,}600 .$$

so that

$$\frac{f_a}{f_A} = 0.0785$$

Also

$$f_t = \frac{25000}{2 \times 0.7518} = 16,630$$

and, from equation (11),

$$f_T = 96,330$$

so that

$$\frac{f_t}{f_T} = 0.1726$$

The allowable value of f_b/f_B may now be obtained from equation (14). Substituting in the values just found for f_a/f_A and f_t/f_T and solving for f_b/f_B gives

$$\frac{f_b}{f_B} = 0.893$$

In order to obtain the actual value of f_b, the maximum bending moment $\overline{M}$ must be known. By elastic theory (see appendix B, equation (33)) for the given conditions of loading

$$\frac{M}{M_b} = \sec 52 \sqrt{\frac{16000}{29500000 \times 1.128}} = 2.395$$

and from equation (15)

$$\frac{\overline{M}}{M_b} = 2.824$$

Consequently,

$$f_b = \frac{2.824 \times 54000}{0.7518} = 202,800$$

and, from equation (10),

$$f_B = 228,200$$

so that

$$\frac{f_b}{f_B} = 0.889$$

Since this value is less than the allowable value of 0.893, the 3—inch by 0.120—inch tube is satisfactory.

National Bureau of Standards,
Washington, D. C., October 2, 1942.

APPENDIX A

ESTIMATION OF THE COMPRESSIVE YIELD STRENGTH AND YOUNG'S MODULUS

After the beginning of the investigation, the mechanical properties of a single tube were found to be quite variable along its length and the compressive yield strength, for example, of a single compressive specimen could not be taken as that of other specimens at some distance from it. It was therefore found necessary to do what could be done to estimate the compressive yield strengths of these other specimens.

After the variability was discovered, two compressive specimens were taken from each tube; but unfortunately some tubes had been used up by this time, from each of which only one compressive specimen had been cut. When two compressive specimens existed for a tube, the

moduli of elasticity and the yield strengths of intermediate specimens were obtained by linear interpolation between the values for the two compressive specimens.

When a tube had only one compressive specimen but also one or more crinkling specimens or a tensile specimen not adjacent to a compressive specimen, the compressive yield strength of the crinkling specimen (or specimens) or of the tensile specimen was estimated by the procedure to be explained. The compressive yield strengths of intermediate specimens were then obtained by linear interpolation, as mentioned in the last paragraph.

The moduli of elasticity and the compressive yield strengths of all specimens between an end of a tube and the nearest specimen for which these quantities were known, or had been estimated, were taken equal to the values for the nearest specimen.

The following procedure was adopted for estimating the compressive yield strengths of crinkling specimens and of tensile specimens not adjacent to compressive specimens. If there were no variation in properties along the length of a tube, the compressive yield strength of such a specimen would be that of the compressive specimen. Denote this yield strength by X. In the case of a crinkling specimen the crinkling strength, f_A, and the ratio of diameter to thickness, d/t, are known. If the modulus of elasticity, E, is assumed to be the same as that of the compressive specimen from the same tube, equation (2) may be solved for the compressive yield strength that the crinkling specimen would have had to have to satisfy equation (2). Denote this yield strength by X'. The "true" yield strength, S, for specimens between the crinkling specimen and the compressive specimen will presumably lie between X and X':

$$S = X \pm x_2 = X' \mp x_2' \qquad (16)$$

Here x_2 and x_2' are corrections to be applied to X and X', respectively, to bring about the equality (16). The values of x_2 and x_2' were determined as follows. Eight sets of observations, on tubes having two compressive specimens each, indicated a maximum variation in compressive yield strength of 184 pounds per square inch per inch. Denote by x_1 the product of 184 and the distance between the middle of the compressive specimen and the

middle of the crinkling specimen. The value of x_1 is therefore the maximum value by which the yield strength of the crinkling specimen may be expected to depart from that of the compressive specimen. On the other hand, 28 observations on compressive specimens indicated a maximum departure of 0.020 in σ_A from the value given by equation (2). Denote by x_1' the quantity $\frac{0.020}{\sigma_A} X'$. That is, x_1' is approximately the maximum value by which the yield strength of the crinkling specimen may be expected to differ from the yield strength determined for it from equation (2). Now, assume the corrections x_2 and x_2' to be determined from equation (16) and the relation

$$\frac{x_2'}{x_2} = \frac{n_1 x_1'}{n_1' x_1} \tag{17}$$

where n_1 and n_1' are the numbers of observations in the two sets discussed: namely, 8 and 28, respectively. It is reasonable that $\frac{x_2'}{x_2}$ should vary, roughly, inversely as the numbers of observations in the two sets and directly as the maximum errors in the two sets.

The procedure for estimating the compressive yield strength of a tensile specimen not adjacent to a compressive specimen is essentially the same as that just explained. In this case, X' is the yield strength from equation (1), and x_1' is 7350 pounds per square inch, the maximum departure of an observed value from that given by equation (1). There were 17 observations for determining equation (1), so that $n_1' = 17$.

Elimination of x_2 and x_2' from equations (16) and (17) gives

$$S = X \frac{1 + \frac{n_1' x_1 X'}{n_1 x_1' X}}{1 + \frac{n_1' x_1}{n_1 x_1'}} \tag{18}$$

The application of the procedure to a specific case will be illustrated. The modulus of elasticity and the compressive yield strength of specimen 1HD-C were 29,040,000 and 183,700 pounds per square inch, respectively. The crinkling strength of specimen 1HD-A was 179,700 pounds per square inch and its ratio of diameter to thickness was 30.80. If $f_A = 179,700$, $E = 29,040,000$, and $d/t = 30.80$ are substituted in equation (2) and the equation is solved for the compressive yield strength, it is found to be 172,700 pounds per square inch. The corresponding value of σ_A is 1.041. Put

$$X = 183,700$$

$$X' = 172,700$$

The distance between specimens 1HD-C and 1HD-A was 44.75 inches and therefore $x_1 = 184 \times 44.75 = 8234$. The value of x_1' is $x_1' = \frac{0.020}{1.041} \times 172,700 = 3318$; $n_1 = 8$, and for the crinkling specimen $n_1' = 28$. Substitution of all these quantities in equation (18) and simplifying gives $S = 173,800$.

APPENDIX B

ELASTIC DEFLECTION OF BEAMS UNDER COMBINED LOAD

Suppose that a beam is loaded axially by equal and opposite compressive forces P and further that other forces, such as transverse forces, are applied to bend the beam. Then, the bending moment M at any cross section may be written as

$$M = M_x - Py \tag{19}$$

where M_x is the portion of the moment produced by other than the axial load, and y is the deflection. The equation of the elastic curve of the beam is

$$EI \frac{d^2y}{dx^2} = M \tag{20}$$

where I is the least moment of inertia of the cross-sectional area about an axis normal to the plane of bending, and x is measured in the longitudinal direction of the beam. From equations (19) and (20)

$$\frac{d^2y}{dx^2} + \frac{P}{EI}y = \frac{M_x}{EI}$$

or, with $\frac{P}{EI} = \alpha^2$

$$\frac{d^2y}{dx^2} + \alpha^2 y = \frac{M_x}{EI} \tag{21}$$

If the beam is of uniform cross section, the integral of equation (21) may be written in the form

$$y = \frac{M_x}{P} + C_1 \sin \alpha x + C_2 \cos \alpha x$$

$$- \frac{1}{P}\left(\sin \alpha x \int \sin \alpha x \frac{dM_x}{dx}\,dx + \cos \alpha x \int \cos \alpha x \frac{dM_x}{dx}\,dx\right) \tag{22}$$

from which

$$\frac{dy}{dx} = \frac{1}{P}\frac{dM_x}{dx} + C_1\alpha \cos \alpha x - C_2\alpha \sin \alpha x$$

$$- \frac{1}{P}\left(\cos \alpha x \int \cos \alpha x \frac{d^2M_x}{dx^2}\,dx + \sin \alpha x \int \sin \alpha x \frac{d^2M_x}{dx^2}\,dx\right) \quad (23)$$

where the arbitrary constants of integration, C_1 and C_2, are to be determined from the boundary conditions. Equation (22) may also be written

$$M = -C_1 P \sin \alpha x - C_2 P \cos \alpha x + \sin \alpha x \int \sin \alpha x \frac{dM_x}{dx}\,dx + \cos \alpha x \int \cos \alpha x \frac{dM_x}{dx}\,dx \quad (24)$$

It may be noted that the parentheses in equations (22) and (23) and the sum of the last two terms of equation (24) become zero if M_x is a linear function of x.

The constants of integration for a few conditions of loading will be determined. First take the symmetrical case of the tests: namely, two equal transverse loads each situated a distance $k\frac{l}{2}$ from the nearer support, where $0 \leqq k \leqq 1$, and l is the length of the beam. M_x is everywhere linear in x, and from equations (22) and (23) if M_b denotes the maximum moment produced by the transverse loads and the origin is taken at one end of the beam,

for $0 \leqq x \leqq k\frac{l}{2}$,

$$y = \frac{2M_b x}{Pkl} + C_1' \sin \alpha x - C_2' \cos \alpha x \quad (25)$$

$$\frac{dy}{dx} = \frac{2M_b}{Pkl} + C_1' \alpha \cos \alpha x - C_2' \alpha \sin \alpha x \quad (26)$$

for $k\frac{l}{2} \leqq x \leqq \left(1 - \frac{k}{2}\right)l$,

$$y = \frac{M_b}{P} + C_1 \sin \alpha x + C_2 \cos \alpha x \qquad (27)$$

$$\frac{dy}{dx} = C_1 \alpha \cos \alpha x - C_2 \alpha \sin \alpha x \qquad (28)$$

When $x = 0$, $y = 0$; and therefore $C_2' = 0$. When $x = k\frac{l}{2}$, $y_{\text{equation}(25)} = y_{\text{equation}(27)}$, and $\left(\frac{dy}{dx}\right)_{\text{equation}(26)} = \left(\frac{dy}{dx}\right)_{\text{equation}(28)}$. Moreover, when $x = \frac{l}{2}$, $\frac{dy}{dx} = 0$. These conditions give

$$C_1' \sin k\frac{l}{2}\alpha = C_1 \sin k\frac{l}{2}\alpha + C_2 \cos k\frac{l}{2}\alpha$$

$$\frac{2M_b}{Pkl} + C_1' \alpha \cos k\frac{l}{2}\alpha = C_1 \alpha \cos k\frac{l}{2}\alpha - C_2 \alpha \sin k\frac{l}{2}\alpha$$

$$0 = C_1 \cos \frac{l}{2}\alpha - C_2 \sin \frac{l}{2}\alpha$$

Elimination of C_1' from these equations, and solution for C_1 and C_2 give

$$C_1 = -\frac{2M_b}{Pkl\alpha} \sin k\frac{l}{2}\alpha \tan \frac{l}{2}\alpha$$

$$C_2 = -\frac{2M_b}{Pkl\alpha} \sin k\frac{l}{2}\alpha$$

The maximum bending moment occurs at the middle of the beam, and when the values just found for C_1 and C_2, together with $x = \frac{l}{2}$, are substituted in equation (24), the maximum value for $\frac{M}{M_b}$ assuming elastic action, is

$$\frac{M}{M_b} = \frac{\sin k\frac{l}{2}\sqrt{\frac{P}{EI}}}{k\frac{l}{2}\sqrt{\frac{P}{EI}} \cos \frac{l}{2}\sqrt{\frac{P}{EI}}} \qquad (29)$$

It is from this equation that the abscissas of the points of figure 18 were computed.

For the case of a beam carrying a single concentrated load at the middle, $k = 1$:

$$\frac{M}{M_b} = \frac{\tan \frac{l}{2}\sqrt{\frac{P}{EI}}}{\frac{l}{2}\sqrt{\frac{P}{EI}}} \tag{30}$$

For the case of a beam loaded by couples at the ends, $k = 0$:

$$\frac{M}{M_b} = \sec \frac{l}{2}\sqrt{\frac{P}{EI}} \tag{31}$$

If l is replaced by $2l$ in equation (30), the case of a cantilever beam loaded by a concentrated force at the free end is obtained:

$$\frac{M}{M_b} = \frac{\tan l\sqrt{\frac{P}{EI}}}{l\sqrt{\frac{P}{EI}}} \tag{32}$$

If l is replaced by $2l$ in equation (31), the case of a cantilever beam loaded by a couple at the free end is obtained:

$$\frac{M}{M_b} = \sec l\sqrt{\frac{P}{EI}} \tag{33}$$

Finally, the maximum value of M/M_b for a uniformly loaded beam will be determined. In terms of the maximum moment M_b produced by the transverse load

$$M_x = 4M_b \frac{x}{l}\left(1 - \frac{x}{l}\right)$$

Equation (22) becomes

$$y = \frac{4M_b}{P}\frac{x}{l}\left(1 - \frac{x}{l}\right) + C_1 \sin \alpha x + C_2 \cos \alpha x + \frac{8M_b}{P l^2 \alpha^2}$$

and for the determination of C_1 and C_2 when $x = 0$ or l, $y = 0$:

$$C_2 = -\frac{8M_b}{Pl^2\alpha^2},$$

$$C_1 = -\frac{8M_b}{Pl^2\alpha^2}\frac{1 - \cos \alpha l}{\sin \alpha l}$$

The maximum value of M/M_b is at the middle of the beam, and substitution in equation (24) of the values of C_1 and C_2 just found, together with $x = \frac{l}{2}$, gives

$$\frac{M}{M_b} = \frac{8EI}{Pl^2}\left(\sec \frac{l}{2}\sqrt{\frac{P}{EI}} - 1\right) \qquad (34)$$

REFERENCES

1. Osgood, William R.: The Crinkling Strength and the Bending Strength of Round Aircraft Tubing. Rep. No. 632, NACA, 1938.

2. Lundquist, Eugene E., and Schwartz, Edward B.: The Critical Compression Load for a Universal Testing Machine when the Specimen is Loaded through Knife Edges. T.N. No. 860, NACA, 1942.

3. Tuckerman, L. B.: Discussion of paper by R. L. Templin, "The Determination and Significance of the Proportional Limit in the Testing of Metals." A.S.T.M. Proc., vol. 29, pt. II, 1929, pp. 538–546.

4. Osgood, W. R.: A Rational Definition of Yield Strength. Jour. Appl. Mech., vol. 7, no. 2, June 1940, pp. A–61 – A–62.

5. Geckeler, J. W.: Plastisches Knicken der Wandung von Hohlzylindern und einige andere Faltungserscheinungen an Schalen und Blechen. Z.f.a.M.M., Bd. 8, Heft 5, Oct. 1928, pp. 341–352.

6. Stang, Ambrose H., Ramberg, Walter, and Back, Goldie: Torsion Tests of Tubes. Rep. No. 601, NACA, 1937.

7. Timoshenko, S.: Theory of Elastic Stability. McGraw-Hill Book Co., Inc., 1936, p. 486.

8. King, H. W.: Handbook of Hydraulics. McGraw-Hill Book Co., Inc., 1939, tables 38 and 39.

TABLE I.- NOMINAL CROSS-SECTIONAL PROPERTIES OF TUBES

Symbol	Outside diameter, d (in.)	Thickness of wall, t (in.)	$\frac{d}{t}$	Cross-sectional area, A (sq in.)	Section modulus, Z ($in.^3$)
L	1	0.065	15.4	0.1909	0.0419
Y	1 1/16	.035	35.7	.1336	.0395
D	1 1/16	.049	30.6	.2234	.0785
F	1 1/16	.065	23.1	.2930	.1008
A	1 1/16	.120	12.5	.5202	.1664

TABLE II.- MECHANICAL PROPERTIES OF TUBES

TENSION					
Specimen	Young's modulus, E (lb/sq in.)	0.002-offset yield strength (lb/sq in.)	5/7 E-secant yield strength (lb/sq in.)	Tensile strength, T (lb/sq in.)	Elongation in 2 in. (percent)
1HL-T	$29,400 \times 10^3$	168,000	168,000	181,000	9
2HL-T	28,700	165,000	165,000	179,000	9
3HL-T	29,200	168,000	168,000	183,000	9
4HL-T	29,000	168,000	169,000	183,000	8
5HL-T	29,100	171,000	171,000	185,000	6
6HL-T	30,000	176,000	176,000	192,000	5
1HY-T	29,300	158,000	158,000	168,000	5
2HY-T	29,400	156,000	156,000	164,000	7
2HY-T1	29,200	172,000	173,000	187,000	5
3HY-T	28,800	181,000	181,000	192,000	5
4HY-T	28,500	175,000	175,000	185,000	—
5HY-T	29,200	170,000	170,000	178,000	6
1HD-T	28,500	167,000	167,000	183,000	7
2HD-T	28,800	163,000	164,000	174,000	5
3HD-T	28,900	167,000	167,000	180,000	5
4HD-T	28,200	161,000	162,000	171,000	11
1HF-T	29,500	173,000	174,000	187,000	7
2HF-T	29,100	169,000	170,000	184,000	6
3HF-T	29,300	167,000	168,000	180,000	7
1HA-T	29,500	155,000	156,000	176,000	—
2HA-T	29,300	159,000	160,000	178,000	8
3HA-T	29,400	161,000	162,000	181,000	8

TABLE II.- MECHANICAL PROPERTIES OF TUBES (Concluded)

COMPRESSION		
Specimen	Young's modulus, E (lb/sq in.)	5/7 E-secant yield strength (lb/sq in.)
1HL-C	$29,800 \times 10^3$	179,000
1HL-C1	29,800	173,000
2HL-C	29,600	175,000
2HL-C1	29,800	179,000
3HL-C	29,200	176,000
3HL-C1	29,500	174,000
4HL-C	29,700	182,000
5HL-C	30,000	179,000
6HL-C	29,800	186,000
1HY-C	30,000	186,000
2HY-C	29,900	188,000
3HY-C	29,400	190,000
4HY-C	29,300	196,000
5HY-C	29,200	173,000
1HD-C	29,000	184,000
2HD-C	29,300	172,000
2HD-C1	28,700	182,000
3HD-C	28,900	177,000
3HD-C1	29,200	185,000
4HD-C	28,900	181,000
4HD-C1	29,200	182,000
1HF-C	29,400	188,000
2HF-C	29,800	184,000
3HF-C	29,200	171,000
3HF-C1	29,300	173,000
1HA-C	29,900	170,000
1HA-C1	29,800	166,000
2HA-C	30,100	171,000
3HA-C	29,300	169,000

TABLE III.- AXIAL TESTS

Specimen	$\frac{d}{t}$	Crinkling strength, f_A (lb/sq in.)	$\frac{l}{\delta} = \frac{Et}{Sd_m}$	$\sigma_A = \frac{f_A}{S}$
3HA-C	12.11	194,600	15.64	1.154
1HA-C1	12.25	191,000	15.96	1.151
1HA-C	12.29	194,700	15.56	1.144
2HA-C	12.33	198,800	15.49	1.160
2HA-A2	12.33	200,800	15.14	1.145
2HA-A3	12.33	200,800	15.11	1.143
2HL-C	15.23	194,100	11.92	1.112
5HL-C	15.26	200,100	11.77	1.119
3HL-C	15.27	194,300	11.61	1.102
4HL-C	15.28	204,300	11.40	1.120
1HL-A1	15.30	198,900	11.85	1.129
1HL-A	15.31	195,200	11.71	1.096
1HL-C	15.31	198,300	11.65	1.108
1HL-C1	15.32	192,300	12.06	1.114
3HL-C1	15.35	194,700	11.82	1.118
2HL-C1	15.40	195,300	11.57	1.093
6HL-C	15.40	204,300	11.15	1.101
2HF-C	22.97	198,800	7.36	1.079
1HF-A1	23.15	197,700	7.21	1.074
1HF-C	23.17	200,100	7.04	1.062
3HF-C	23.23	183,800	7.68	1.074
3HF-C1	23.23	187,900	7.60	1.085
1HF-A	23.23	191,300	7.38	1.068
1HD-A	30.80	179,700	5.61	1.034
3HD-C	30.86	181,000	5.48	1.024
1HD-C	30.86	192,000	5.29	1.045
4HD-C1	30.97	189,700	5.37	1.044
3HD-C1	31.03	194,000	5.24	1.048
2HD-C	31.05	177,700	5.67	1.034
2HD-C1	31.10	190,600	5.23	1.046
4HD-C	31.14	186,700	5.31	1.032
5HY-C	34.18	174,600	5.09	1.009
1HY-A	34.30	174,700	5.31	1.028
2HY-C	34.33	188,400	4.78	1.004
4HY-C	34.75	202,000	4.43	1.031
1HY-C	34.90	185,900	4.77	1.001
3HY-C	36.20	189,600	4.40	.998

TABLE IV.- BENDING TESTS

Specimen	$\frac{d}{t}$	Modulus of rupture f_B (lb/sq in.)	$\frac{l}{\delta} = \frac{Et}{Sd_m}$	$\sigma_B = \frac{f_B d_m}{Sd}$
1HA-B	12.29	256,000	15.56	1.382
1HA-B1	12.30	256,900	15.70	1.402
1HA-B2	12.31	255,600	15.82	1.410
1HL-B2	15.28	248,100	11.89	1.320
1HL-B1	15.31	241,700	11.74	1.272
1HL-B	15.31	248,600	11.65	1.297
5HL-B	15.40	256,300	11.65	1.340
6HL-B	15.40	247,400	11.15	1.246
2HF-B1	23.06	234,200	7.33	1.216
2HF-B2	23.06	232,500	7.33	1.207
2HF-B	23.06	220,200	7.33	1.144
1HF-B2	23.17	241,100	7.20	1.253
1HF-B	23.18	246,400	7.03	1.251
3HF-B	23.23	236,400	7.64	1.314
3HF-B2	23.23	228,800	7.60	1.264
3HF-B1	23.23	228,200	7.60	1.261
1HF-B1	23.23	235,300	7.31	1.245
1HD-B	30.90	226,200	5.29	1.191
1HD-B1	30.97	218,500	5.57	1.217
4HD-B	30.97	220,900	5.37	1.176
2HD-B	31.05	228,600	5.37	1.236
2HD-B1	31.10	220,500	5.23	1.170
2HY-B	34.21	236,000	4.83	1.231
2HY-B1	34.25	230,200	4.87	1.211
5HY-B	34.53	217,000	5.04	1.217
3HY-B	36.10	211,100	4.41	1.080

TABLE V.— TORSIONAL TESTS

Specimen	$\frac{d}{t}$	Modulus of rupture f_T (lb/sq in.)	$\frac{1}{\delta_s} = \left(\frac{E}{S}\right)^{\frac{2}{3}} \frac{t}{d_m}$	$\tau_T = \frac{f_T d_m}{Sd}$
1HA—To1	12.29	109,600	2.787	0.595
1HA—To2	12.31	116,800	2.799	.641
1HA—To	12.31	111,900	2.773	.604
5HL—To	15.26	110,700	2.134	.579
1HL—To2	15.28	114,200	2.155	.611
1HL—To1	15.30	108,600	2.136	.574
1HL—To	15.31	112,700	2.117	.588
1HF—To1	23.15	106,600	1.334	.558
1HF—To	23.16	102,900	1.308	.523
1HF—To2	23.17	101,800	1.327	.529
3HF—To	23.32	91,700	1.369	.507
1HD—To1	30.80	95,800	1.007	.525
3HD—To	30.90	98,300	.975	.514
1HD—To	31.00	92,200	.975	.486
5HY—To	34.18	92,900	.921	.521
2HY—To	34.25	101,800	.891	.533

TABLE VI.- COMBINED AXIAL AND BENDING TESTS

Specimen	$\frac{d}{t}$	Axial stress, f_a (lb/sq in.)	Bending stress, f_b (lb/sq in.)	$\frac{l}{\delta} = \frac{Et}{Sd_m}$	$\sigma_a = \frac{f_a}{S}$	$\sigma_b = \frac{f_b d_m}{Sd}$	$\frac{\sigma_a}{\sigma_A}$	$\frac{\sigma_b}{\sigma_B}$
2HA-AB3	12.30	12,500	227,800	15.15	.071	1.191	.062	.871
2HA-AB2	12.31	39,700	191,400	15.14	.226	1.001	.199	.732
2HA-AB	12.31	4,800	234,500	15.14	.028	1.226	.025	.897
1HL-AB1	15.32	84,500	90,700	12.03	.488	.490	.441	.378
1HL-AB	15.32	43,600	187,400	11.98	.251	1.008	.227	.777
2HF-AB	22.88	52,600	163,500	7.39	.286	.849	.265	.674
2HF-AB1	22.94	58,600	157,700	7.37	.318	.819	.295	.651
1HD-AB	30.74	63,500	132,000	5.62	.366	.735	.352	.606
1HD-AB1	30.86	23,900	209,300	5.60	.138	1.165	.133	.962
1HD-AB2	30.97	48,100	171,600	5.57	.277	.955	.267	.789
2HY-AB1	34.21	142,800	35,800	5.15	.817	.199	.797	.167
2HY-AB4	34.30	125,400	52,200	5.50	.768	.311	.741	.258
2HY-AB3	34.30	120,800	73,100	5.37	.723	.425	.701	.354
2HY-AB2	34.30	117,100	71,800	5.25	.685	.408	.666	.341
2HY-AB	34.30	90,500	92,000	5.01	.505	.498	.495	.420

TABLE VII.- COMBINED BENDING AND TORSIONAL TESTS

Specimen	$\frac{d}{t}$	Bending stress, f_b (lb/sq in.)	Torsional stress, f_t (lb/sq in.)	$\frac{l}{\delta} = \frac{Et}{Sd_m}$	$\frac{l}{\delta_s} = \left(\frac{E}{S}\right)^{\frac{2}{3}} \frac{t}{d_m}$	$\sigma_b = \frac{f_b d_m}{Sd}$	$\tau = \frac{f_t d_m}{Sd}$	$\frac{\sigma_b}{\sigma_B}$	$\frac{\tau}{\tau_T}$
3HA-BT	12.10	218,100	70,800	15.66	2.806	1.186	0.385	0.853	0.621
3HA-BT1	12.10	163,300	99,200	15.66	2.806	.888	.539	.639	.869
3HA-BT2	12.11	39,700	111,400	15.64	2.803	.216	.606	.156	.977
2HA-BT	12.30	217,000	76,200	15.15	2.729	1.135	.398	.830	.646
2HL-BT3	15.23	30,700	111,000	11.92	2.154	.164	.594	.126	1.022
2HL-BT2	15.25	74,900	106,900	11.90	2.150	.401	.572	.309	.985
2HL-BT4	15.27	107,700	103,100	11.80	2.137	.571	.547	.441	.943
3HL-BT	15.30	203,800	74,200	11.58	2.109	1.080	.393	.835	.679
3HL-BT1	15.30	173,100	89,600	11.58	2.109	.918	.475	.709	.820
2HF-BT	23.06	51,100	102,700	7.33	1.346	.265	.533	.211	1.000
2HF-BT1	23.06	77,300	100,500	7.33	1.346	.401	.522	.319	.979
2HF-BT2	23.06	100,900	96,500	7.33	1.346	.524	.501	.417	.940
3HF-BT	23.27	205,800	66,200	7.66	1.381	1.150	.370	.911	.692
3HF-BT1	23.27	172,700	77,600	7.66	1.381	.965	.434	.764	.811
2HD-BT	31.05	94,200	90,100	5.67	1.023	.531	.508	.438	.990
2HD-BT1	31.05	72,400	93,000	5.67	1.023	.408	.524	.336	1.021
2HD-BT2	31.05	48,100	95,300	5.67	1.023	.271	.537	.223	1.047
2HD-BT3	31.05	21,700	93,100	5.56	1.010	.120	.516	.099	1.006
3HD-BT	31.18	181,100	59,100	5.42	.991	.992	.324	.824	.634
3HD-BT1	31.18	161,900	73,100	5.42	.991	.886	.400	.736	.783
3HY-BT5	36.10	181,200	58,900	4.41	.821	.927	.302	.803	.603
3HY-BT4	36.10	153,800	69,200	4.41	.821	.787	.354	.681	.707
3HY-BT3	36.49	101,900	93,700	4.36	.812	.522	.480	.453	.958
3HY-BT2	36.71	80,500	99,600	4.34	.808	.412	.510	.358	1.020
3HY-BT1	36.78	27,600	104,700	4.33	.806	.141	.536	.123	1.072
3HY-BT	36.89	56,100	102,000	4.32	.804	.287	.522	.250	1.044

TABLE VIII.- COMBINED AXIAL, BENDING, AND TORSIONAL TESTS

Specimen	$\frac{d}{t}$	Axial stress, f_a (lb/sq in.)	Bending stress, f_b (lb/sq in.)	Torsional stress f_t (lb/sq in.)	$\frac{l}{\delta} = \frac{Et}{Sd_m}$	$\frac{l}{\delta_s} = \left(\frac{E}{S}\right)^{\frac{2}{3}} \frac{t}{d_m}$	$\sigma_a = \frac{f_a}{S}$	$\sigma_b = \frac{f_b d_m}{Sd}$	$\tau = \frac{f_t d_m}{Sd}$	$\frac{\sigma_a}{\sigma_A}$	$\frac{\sigma_b}{\sigma_B}$	$\frac{\tau}{\tau_T}$
3HA-ABT1	12.20	29,400	197,100	20,200	15.52	2.781	0.174	1.073	0.110	0.152	0.776	0.178
3HA-ABT	12.21	32,700	169,500	40,500	15.50	2.779	.194	.922	.220	.169	.667	.355
4HL-ABT1	15.26	13,800	177,300	43,000	11.41	2.091	.076	.908	.220	.069	.702	.381
4HL-ABT	15.28	4,700	217,600	47,300	11.40	2.088	.026	1.115	.243	.024	.862	.421
2HL-ABT	15.33	18,300	188,900	20,600	11.67	2.118	.103	.993	.108	.093	.767	.186
3HL-ABT	15.33	12,900	197,800	20,800	11.61	2.111	.073	1.051	.111	.066	.812	.192
3HL-ABT2	15.40	1,300	238,600	31,000	11.72	2.121	.007	1.279	.166	.006	.987	.287
3HL-ABT1	15.40	10,600	200,700	31,100	11.64	2.110	.060	1.071	.166	.054	.827	.287
3HF-ABT	23.23	19,100	180,100	39,800	7.60	1.375	.111	.995	.220	.103	.768	.411
4HD-ABT1	30.91	14,800	198,400	30,700	5.36	.987	.082	1.059	.164	.079	.882	.321
3HD-ABT	30.93	53,400	144,600	40,600	5.41	.993	.298	.781	.220	.288	.649	.430
3HD-ABT1	30.99	38,500	203,300	40,200	5.31	.979	.211	1.075	.213	.205	.897	.417
4HD-ABT2	31.03	12,200	202,300	20,500	5.34	.983	.067	1.079	.109	.065	.898	.213
4HD-ABT	31.03	25,200	194,000	30,900	5.32	.981	.140	1.037	.165	.136	.864	.323
4HD-ABT3	31.16	36,100	183,000	20,600	5.33	.980	.199	.975	.110	.193	.812	.215
4HY-ABT	34.71	29,100	171,200	52,500	4.43	.835	.148	.848	.260	.148	.733	.518
4HY-ABT5	34.75	15,000	222,600	22,300	4.43	.835	.077	1.103	.111	.077	.953	.221
4HY-ABT4	34.75	9,600	209,500	44,700	4.43	.835	.049	1.038	.221	.049	.897	.440
4HY-ABT1	34.78	4,300	201,600	22,300	4.43	.834	.022	.999	.110	.022	.863	.219
4HY-ABT3	34.85	24,100	196,200	33,600	4.42	.832	.123	.972	.166	.123	.841	.331
4HY-ABT2	34.97	5,000	221,600	33,600	4.40	.829	.025	1.098	.167	.025	.951	.333

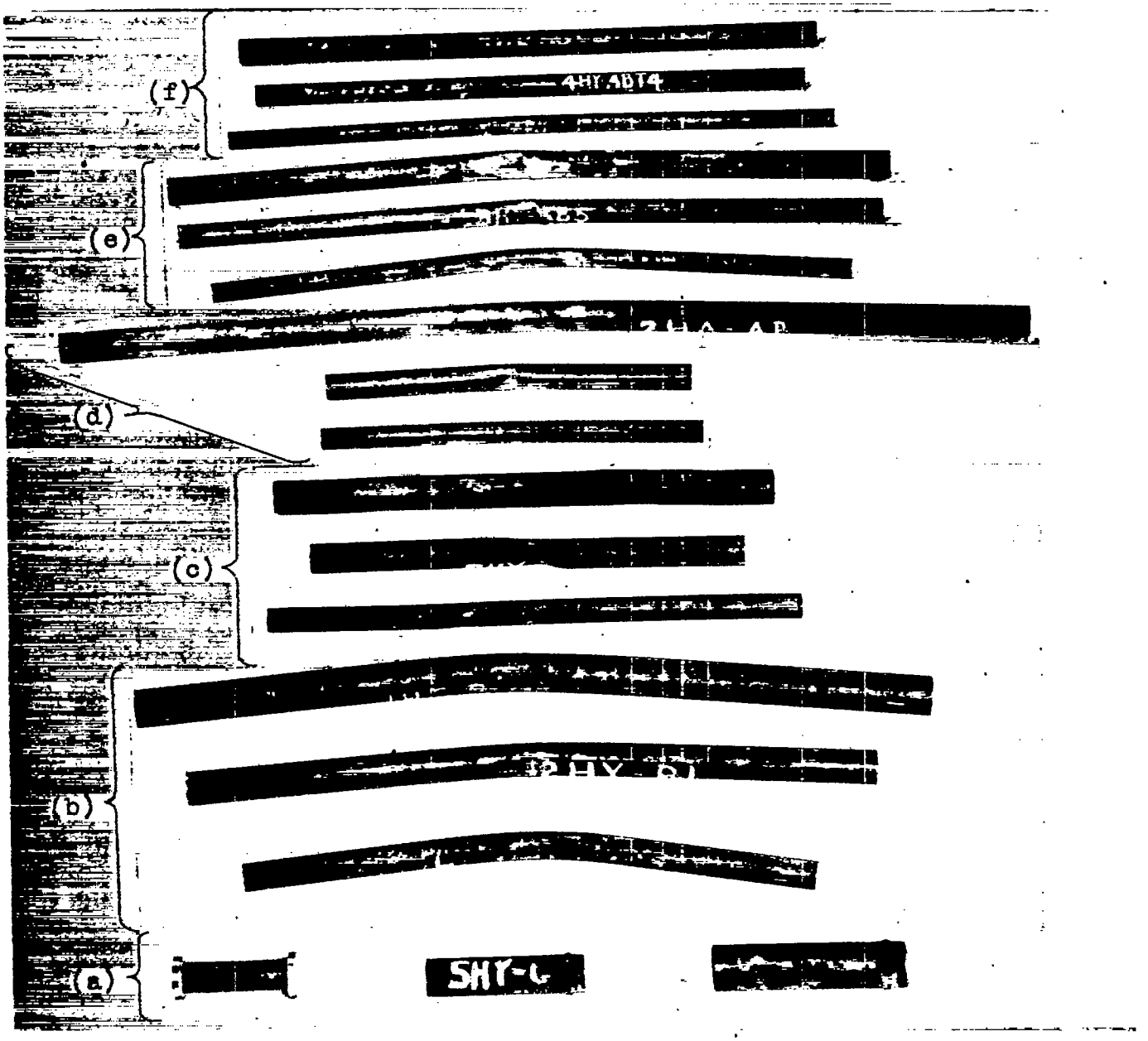

(a) Compressive specimens.
(b) Bending specimens.
(c) Torsional specimens.
(d) Combined axial and bending specimens.
(e) Combined torsional and bending specimens.
(f) Combined axial, bending, and torsional specimens.

Figure 1.— Specimens after testing.

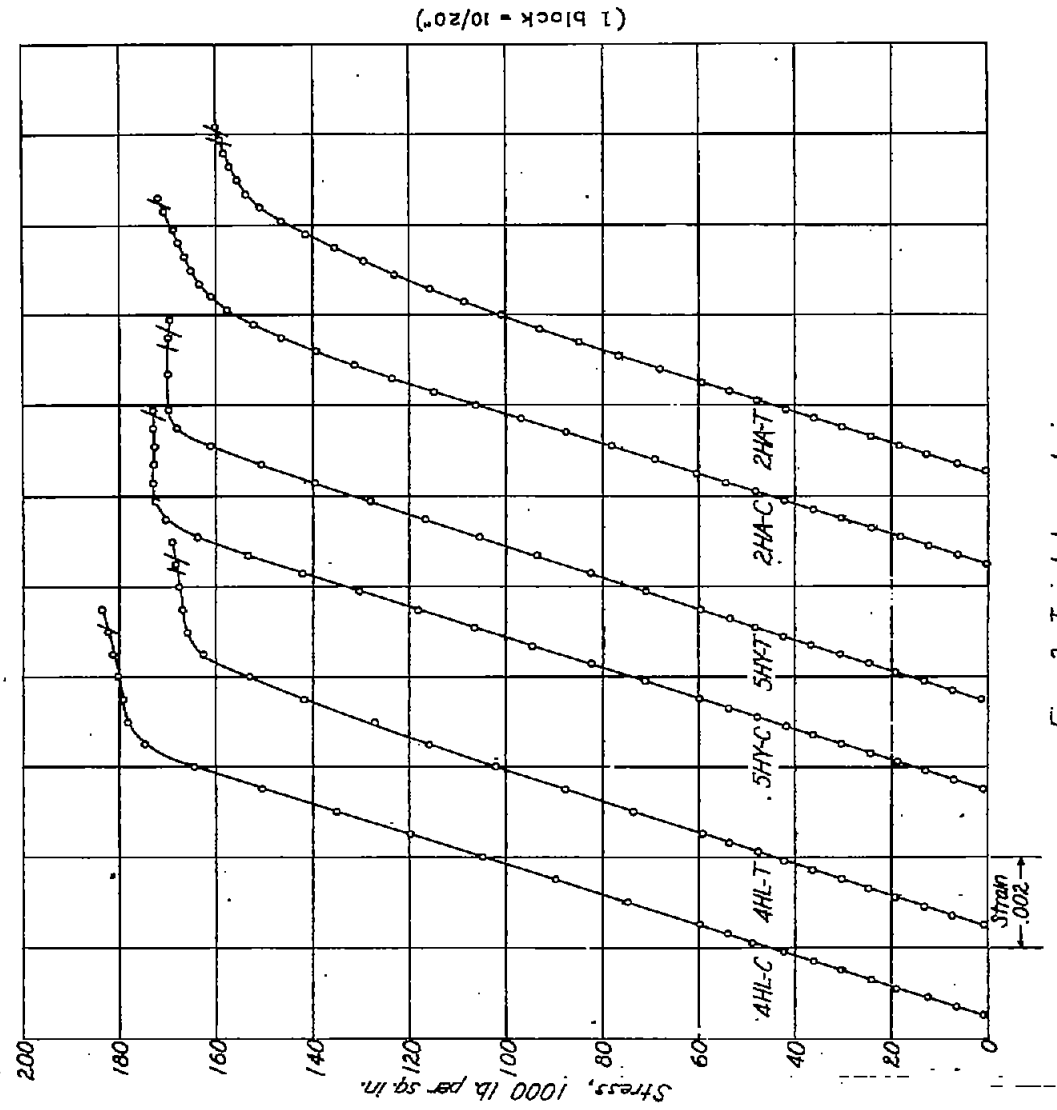

Figure 2.- Typical stress-strain curves.

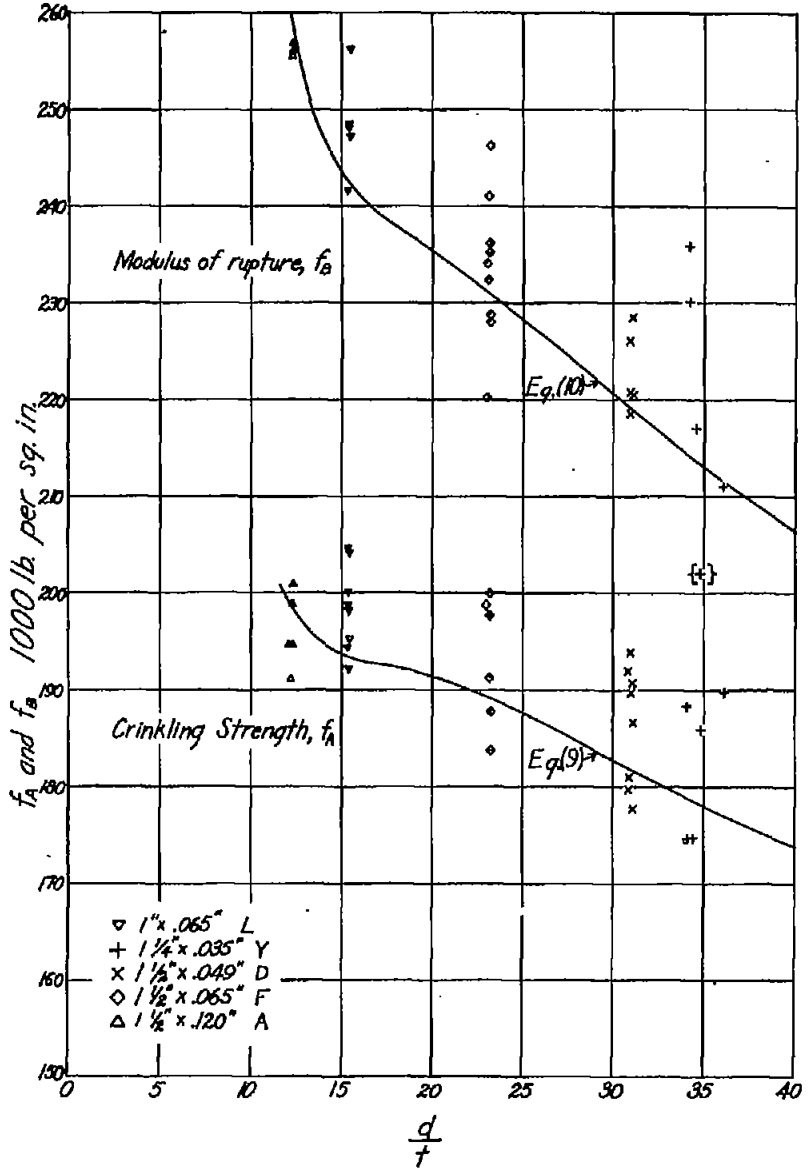

Figure 4.- Variation of f_A and f_B with d/t.

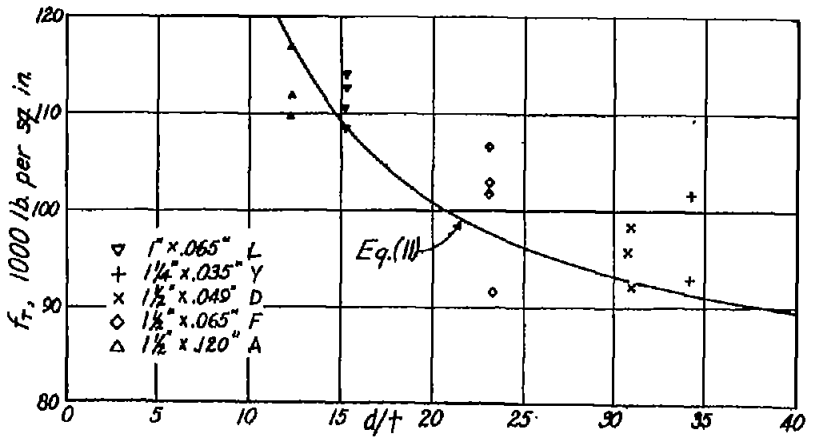

Figure 6.- Variation of f_T with d/t.

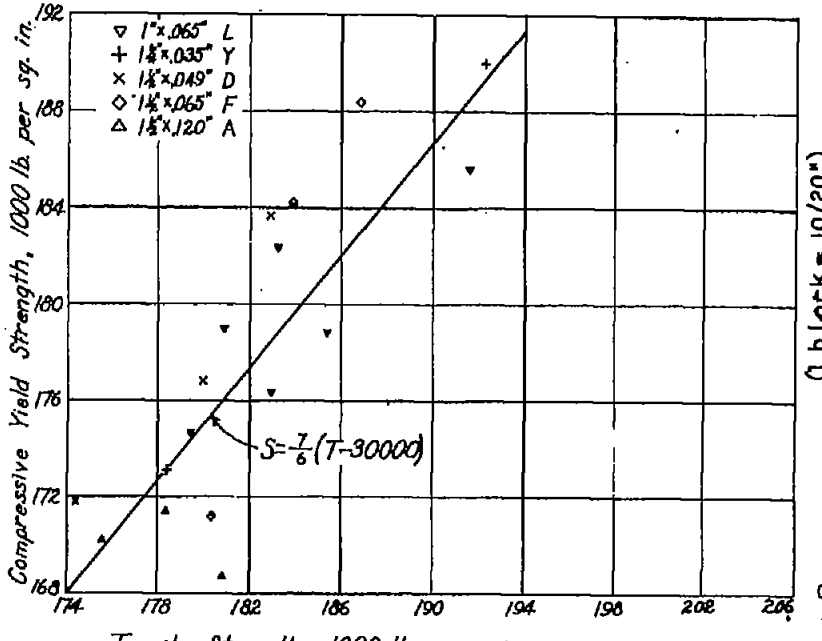

Figure 3.- Relation of compressive yield strength to tensile strength.

(1 block = 10,000 lb.)

Figs. 3,4,6

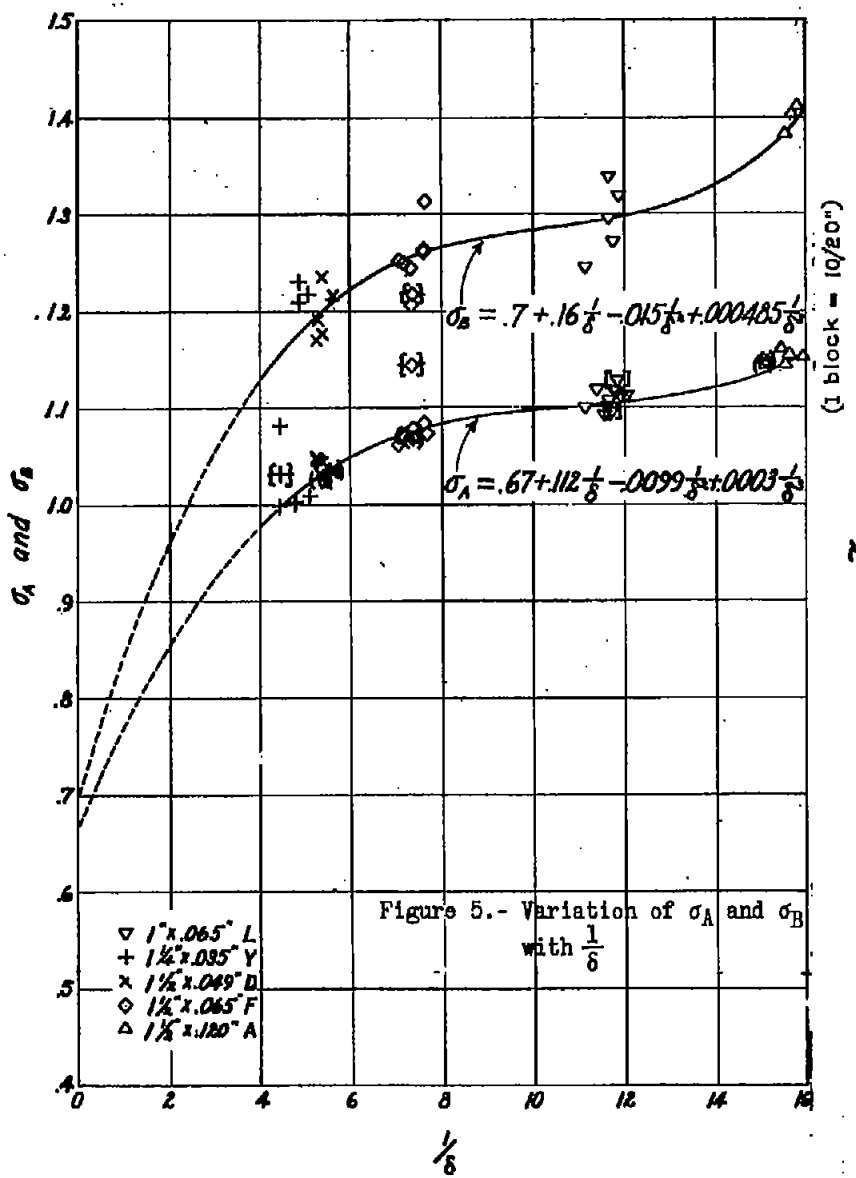

Figure 5.- Variation of σ_A and σ_B with $\frac{1}{\delta}$

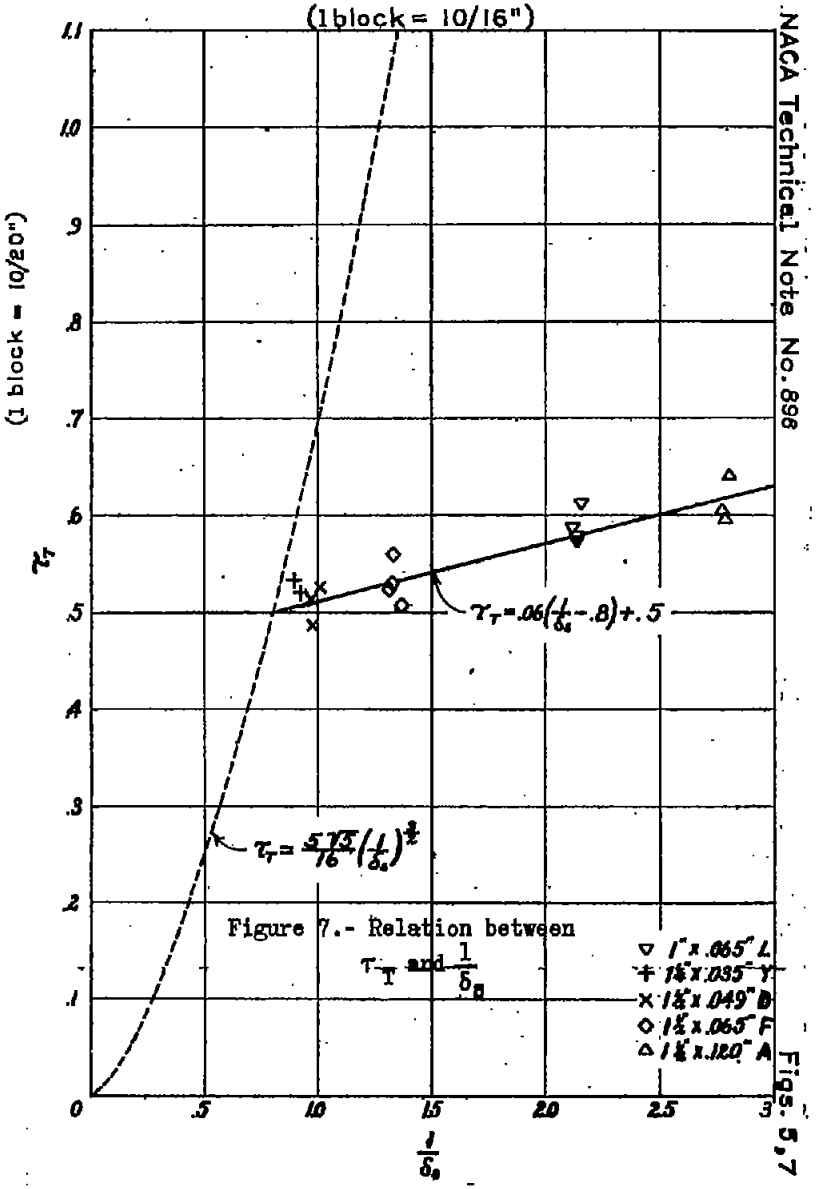

Figure 7.- Relation between τ_T and $\frac{1}{\delta_B}$

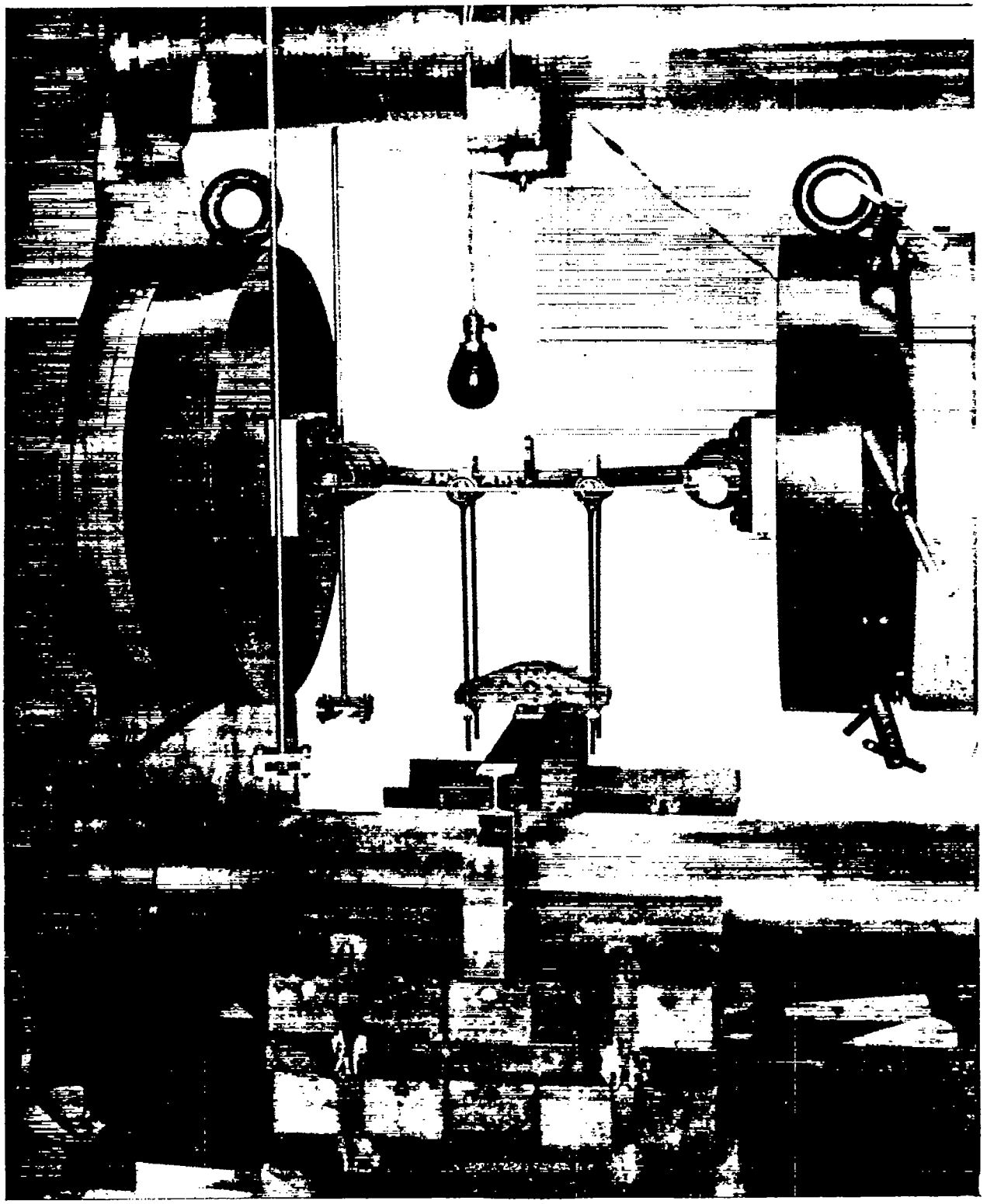

Figure 8.— Test setup for combined axial and bending tests.

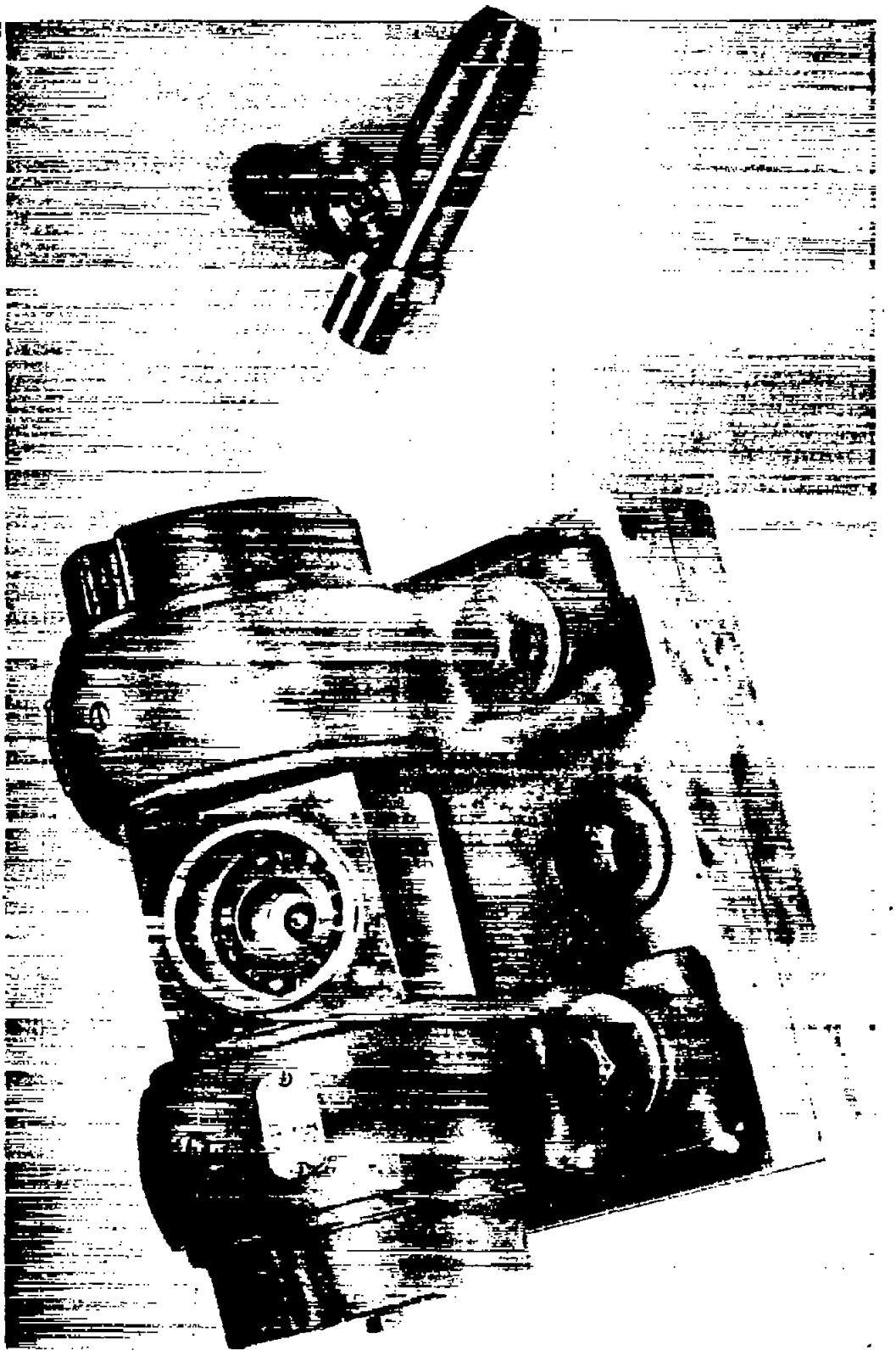

Figure 9.— Pillow block assembly and plugs for combined axial and bending tests.

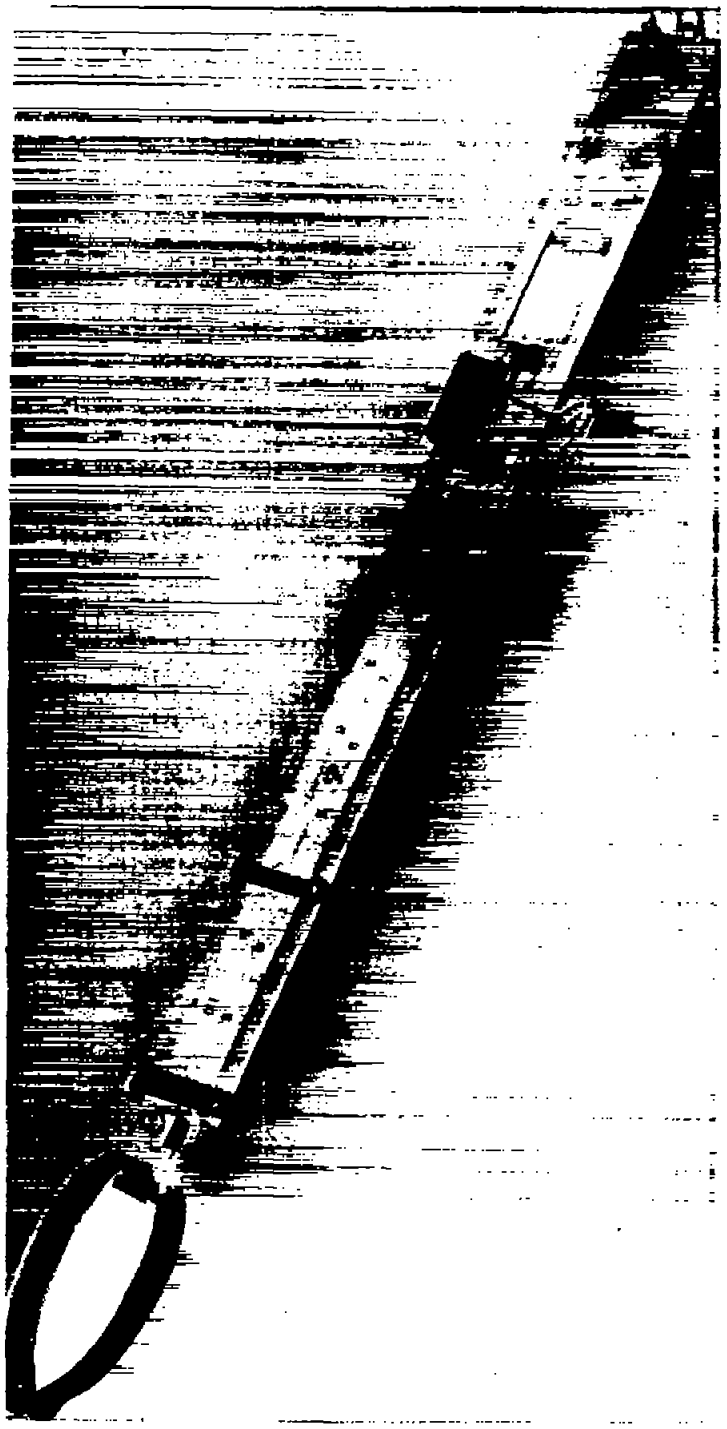

Figure 10.— Deflectometer used in combined axial and bending tests.

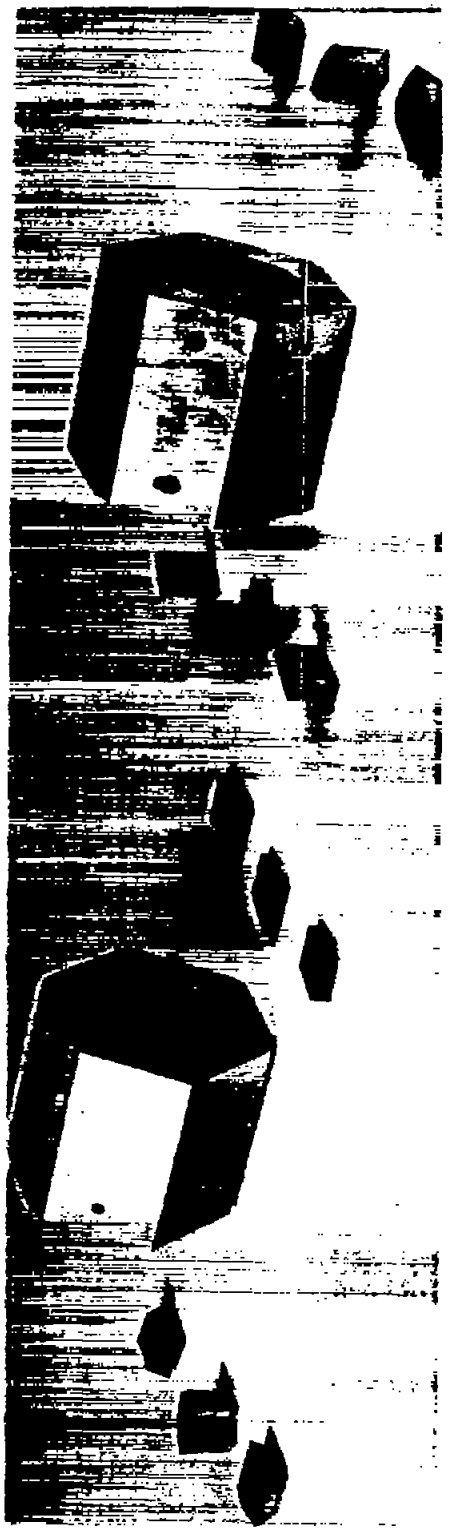

Figure 14.— Grips and plugs used for tests in combined bending and torsion.

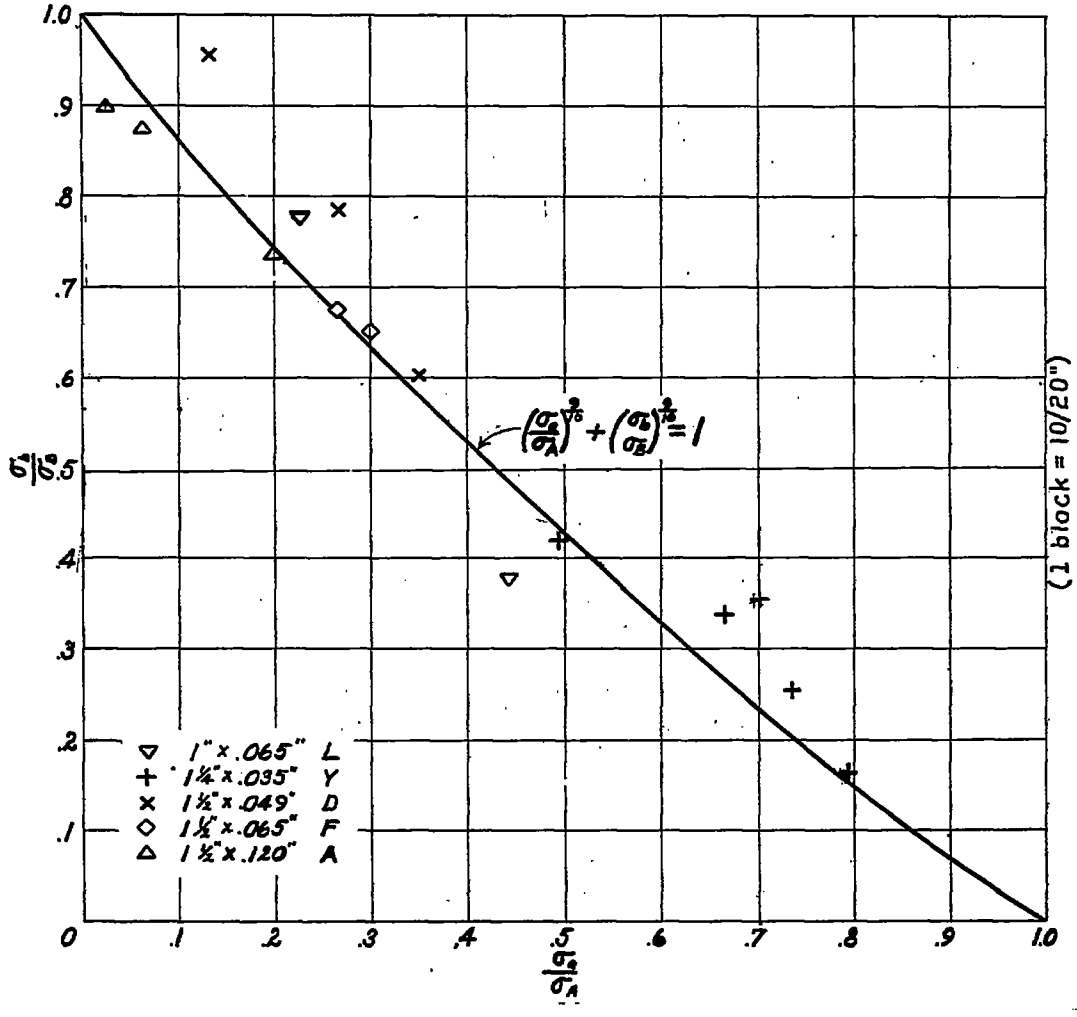

Figure 11.- Relation between $\frac{\sigma_b}{\sigma_B}$ and $\frac{\sigma_a}{\sigma_A}$.

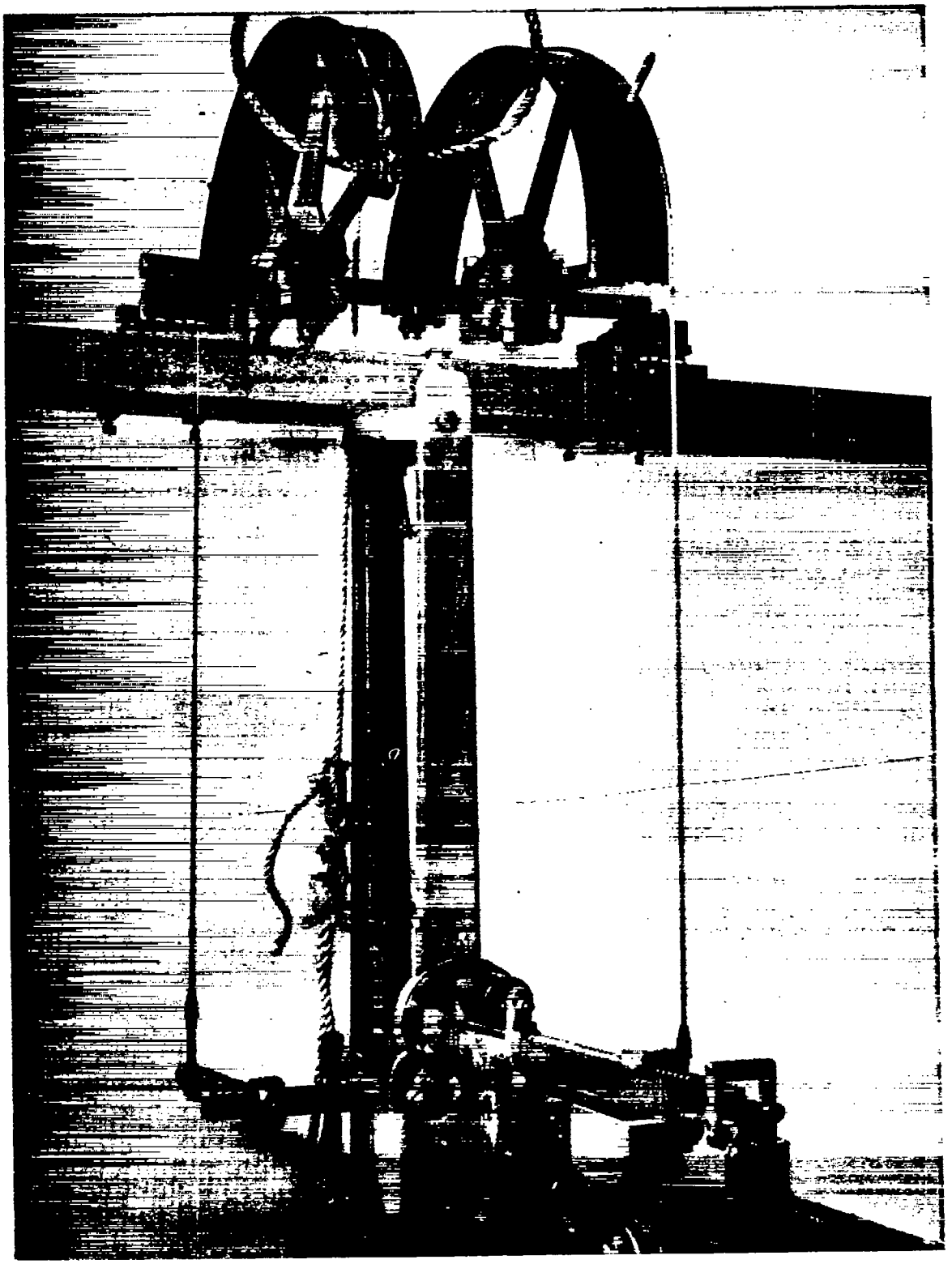

Figure 12.— Setup for combined bending and torsional tests.

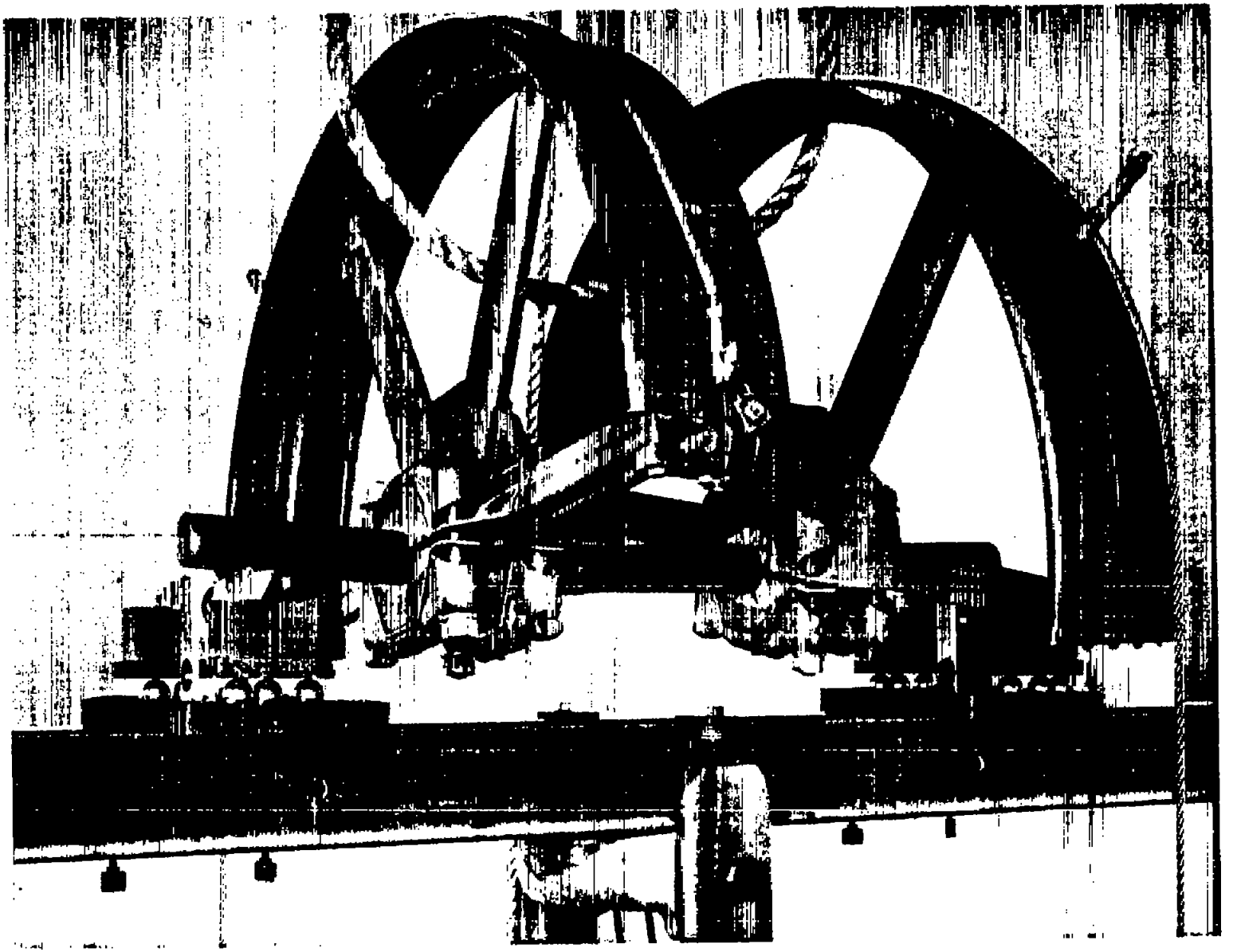

Figure 13.— Detail of test setup for tests in combined bending and torsion.

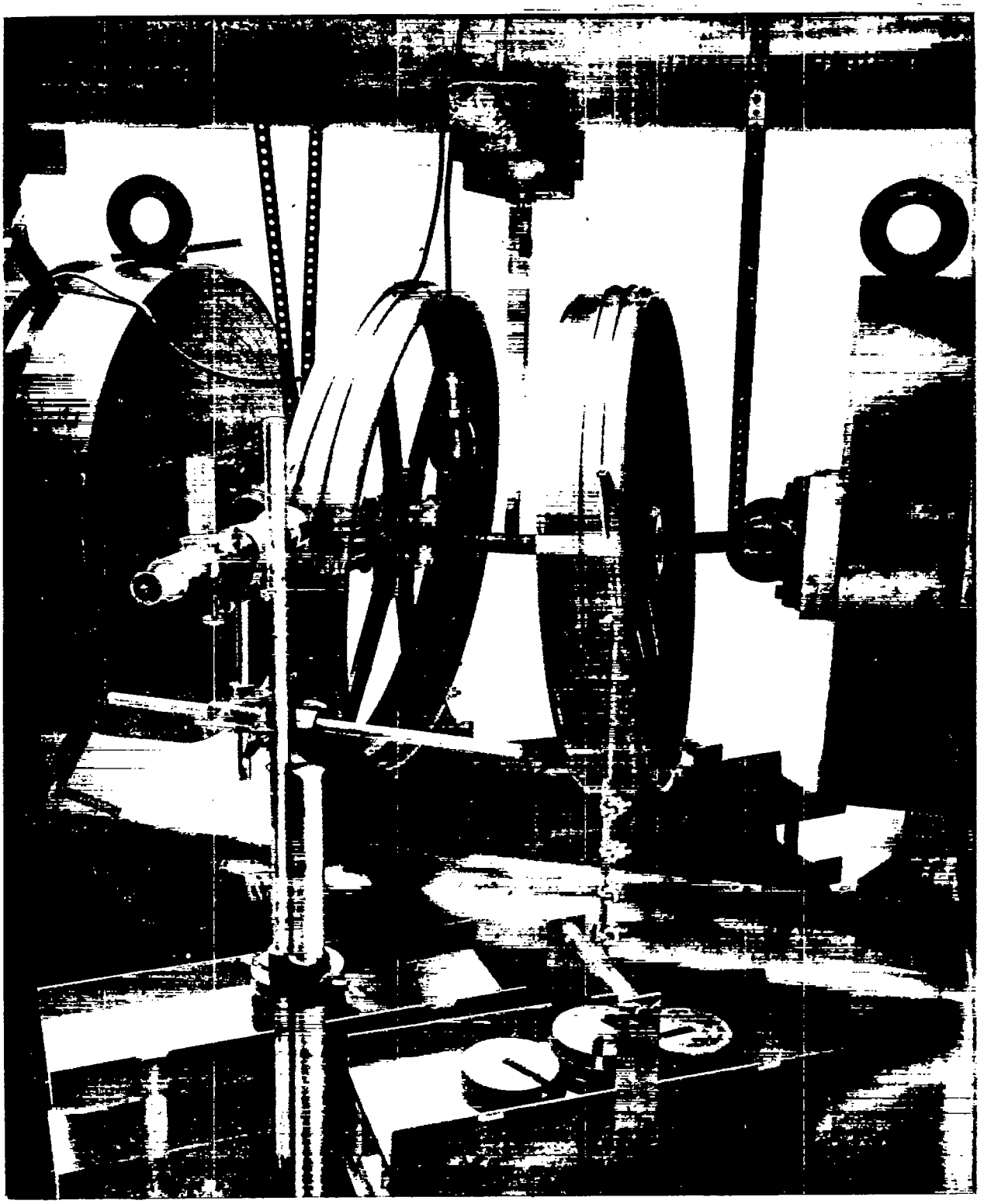

Figure 15.— Setup used in combined axial, bending, and torsional tests.

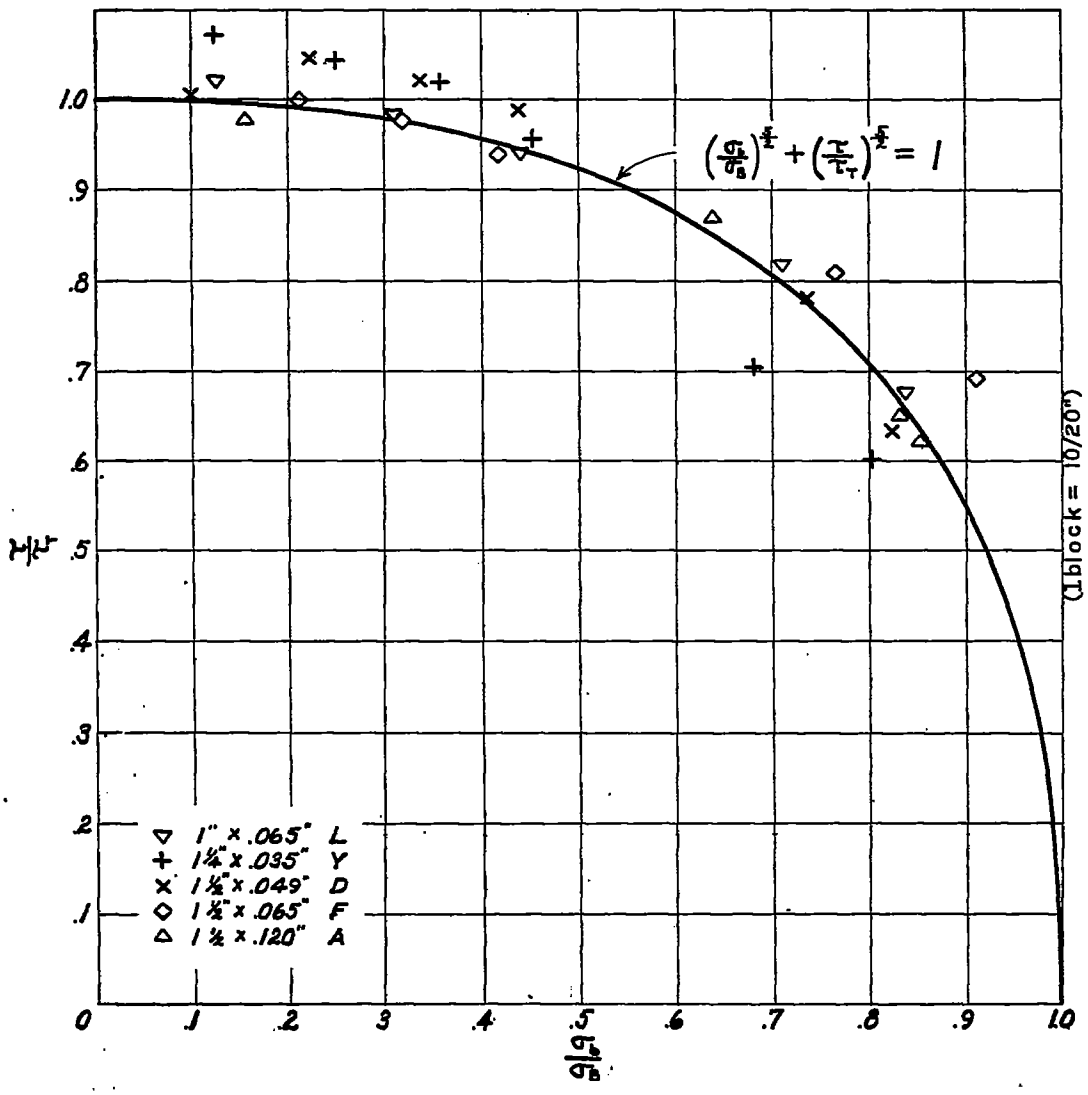

Figure 16.- Variation of $\frac{\tau}{\tau_T}$ with $\frac{\sigma_b}{\sigma_B}$.

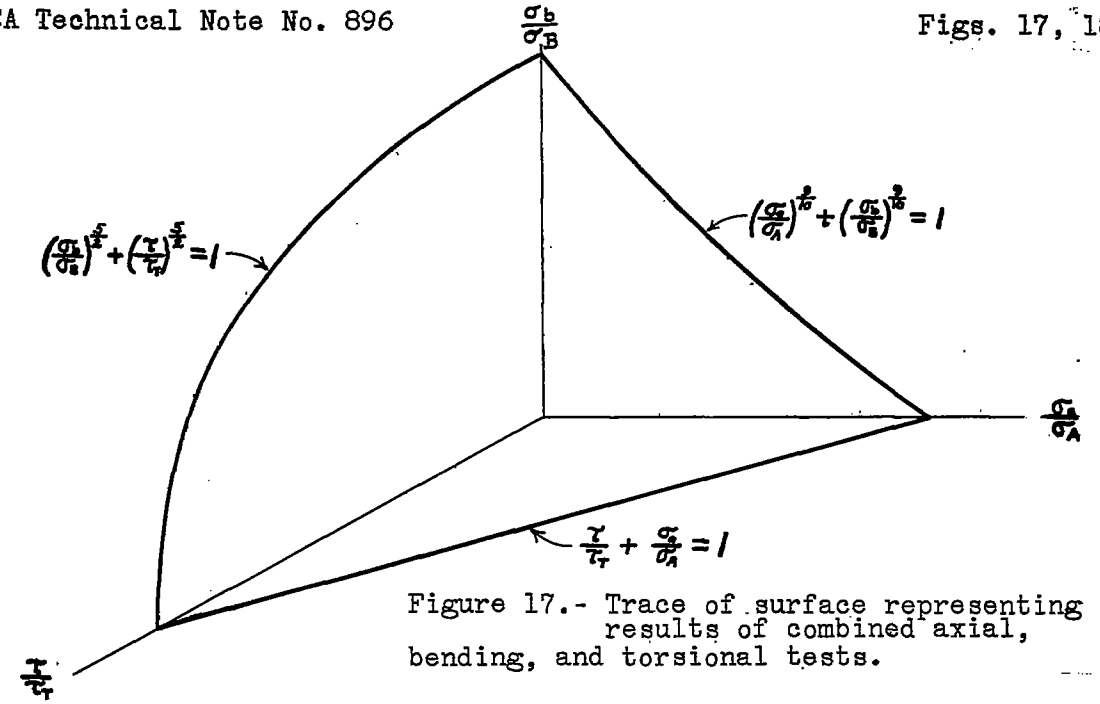

Figure 17.- Trace of surface representing results of combined axial, bending, and torsional tests.

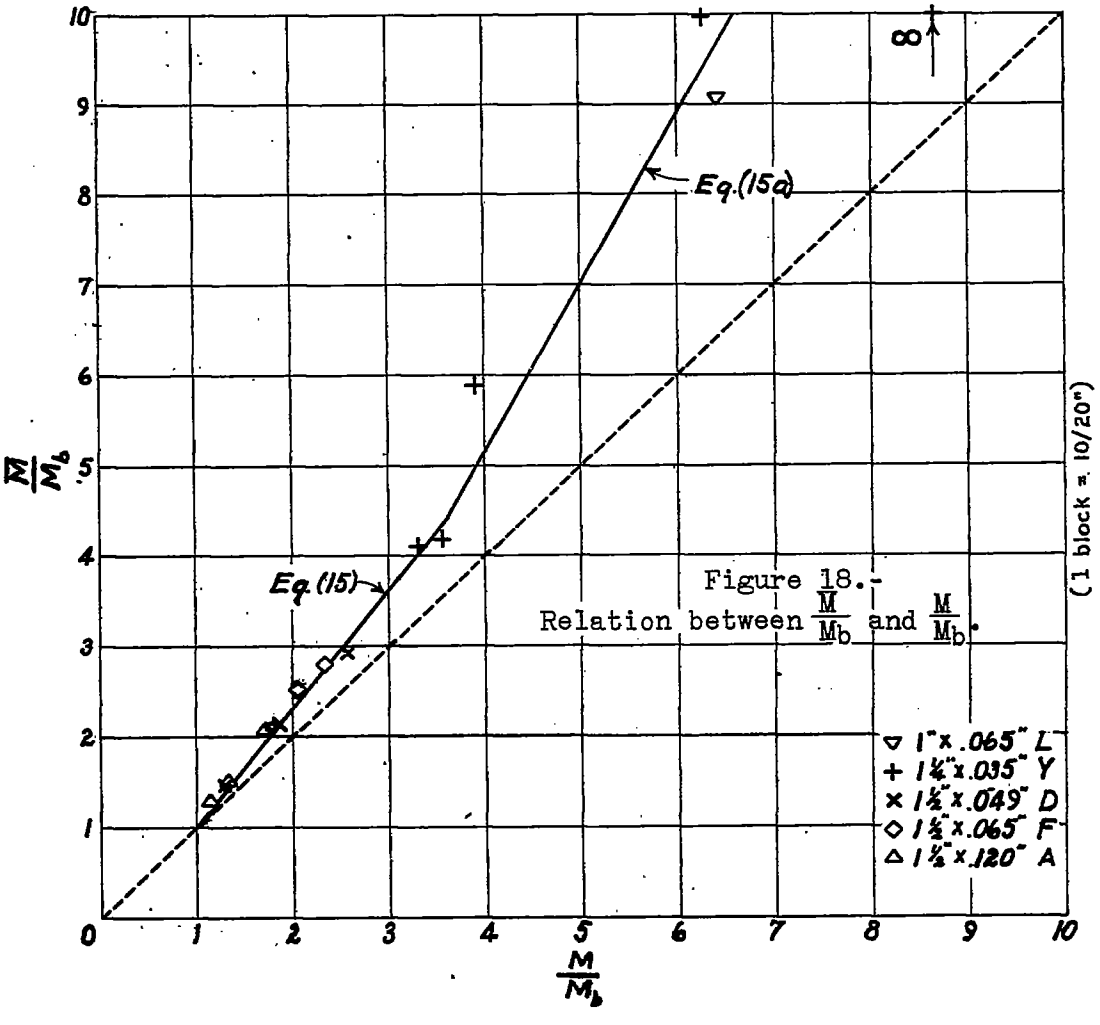

Figure 18.- Relation between $\frac{\overline{M}}{M_b}$ and $\frac{M}{M_b}$.